

# Elliptic Anisotropy at High $p_T$ in pPb Collisions using Subevent Cumulants at CMS



**Rohit Kumar Singh**  
(For the CMS Collaboration)

**Indian Institute of Technology Madras**



**HP2024**  
N A G A S A K I

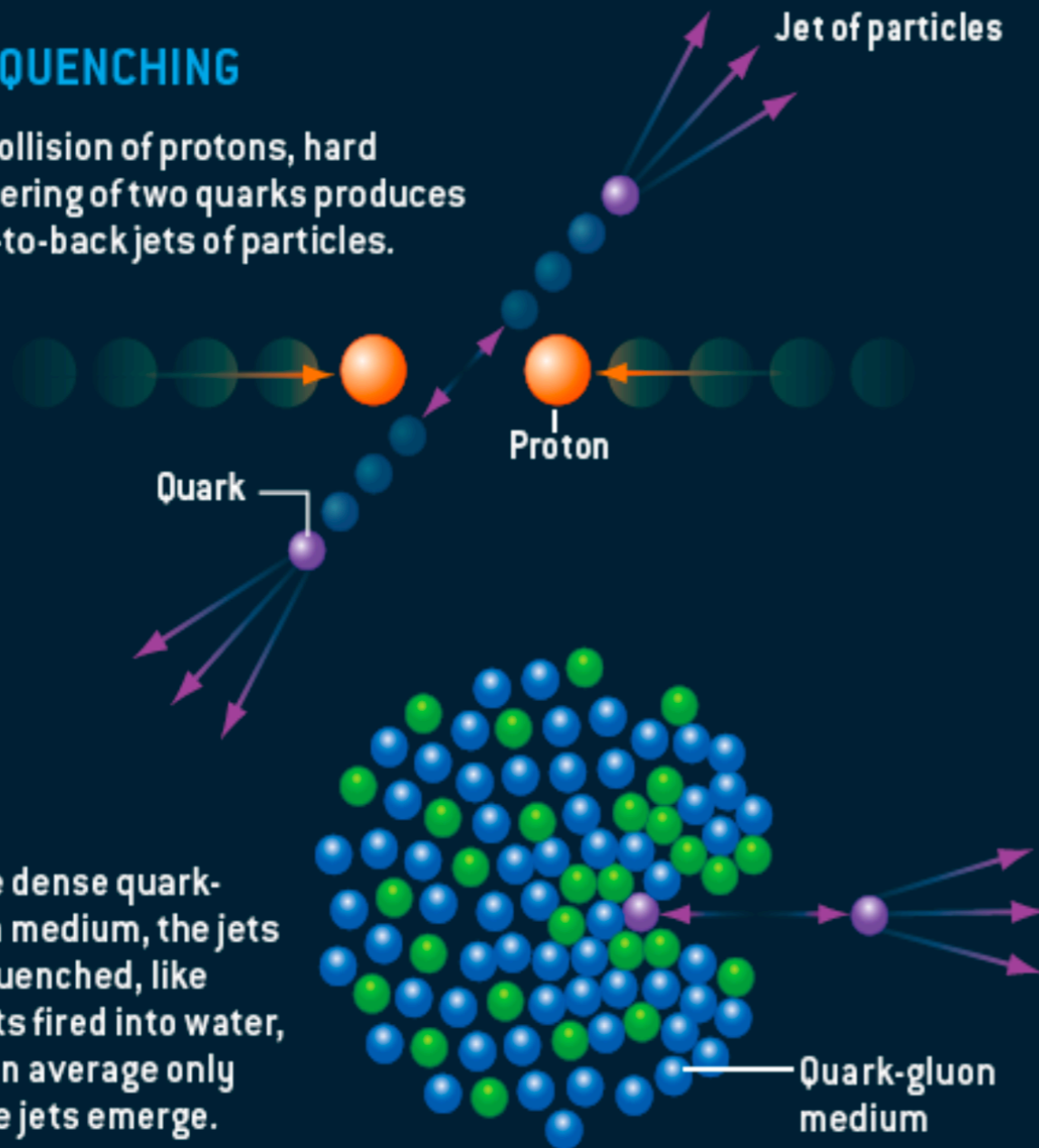
**Date: Sept 23, 2024**

## EVIDENCE FOR A DENSE LIQUID

Two phenomena in particular point to the quark-gluon medium being a dense liquid state of matter: jet quenching and elliptic flow. Jet quenching implies the quarks and gluons are closely packed, and elliptic flow would not occur if the medium were a gas.

### JET QUENCHING

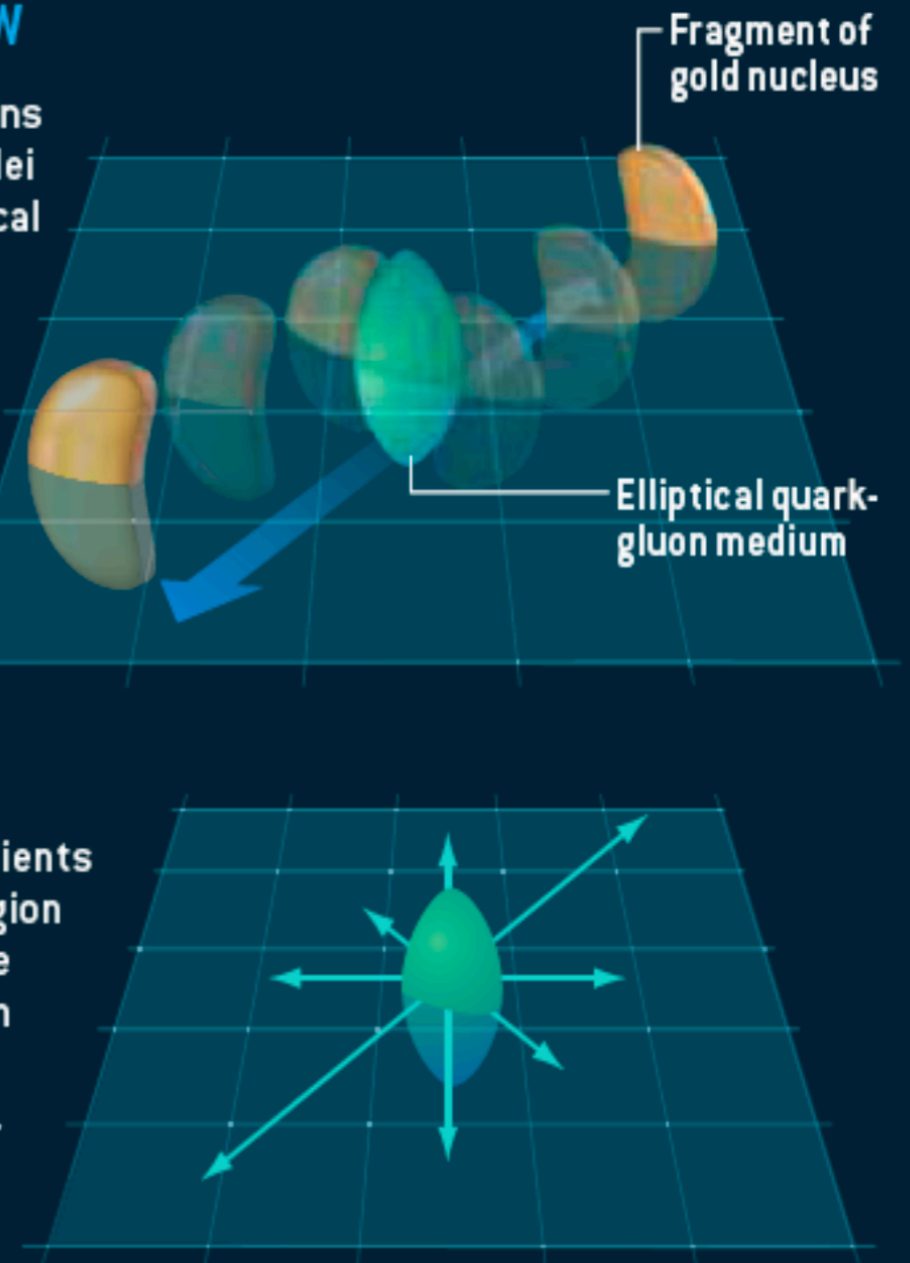
In a collision of protons, hard scattering of two quarks produces back-to-back jets of particles.



### ELLIPTIC FLOW

Off-center collisions between gold nuclei produce an elliptical region of quark-gluon medium.

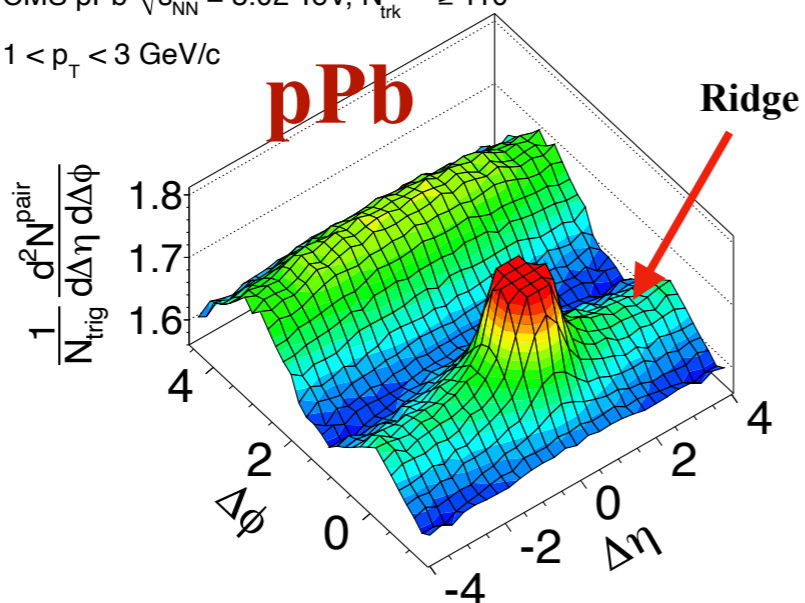
The pressure gradients in the elliptical region cause it to explode outward, mostly in the plane of the collision (*arrows*).



M. Roirdan and W. Zajc  
Scientific American, May 2006

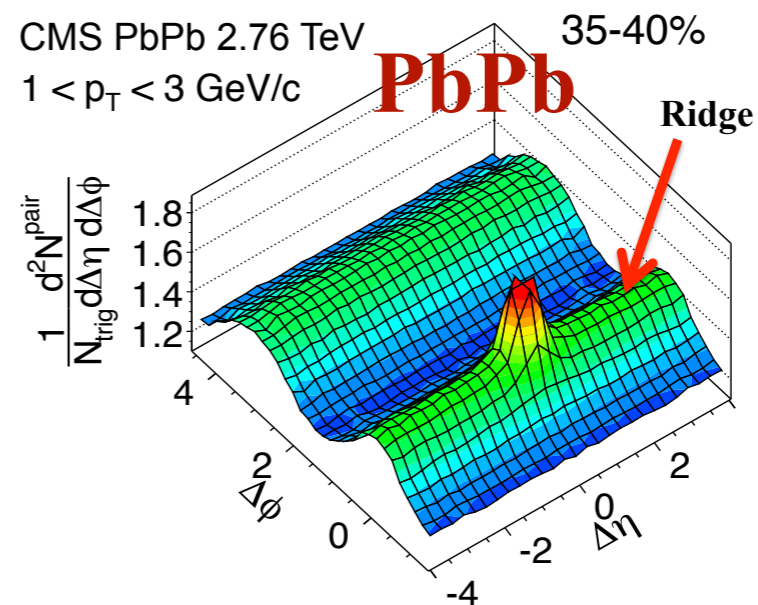
Phys. Lett. B 718, 795 (2013)

CMS pPb  $\sqrt{s_{NN}} = 5.02$  TeV,  $N_{trk}^{offline} \geq 110$   
 $1 < p_T < 3$  GeV/c

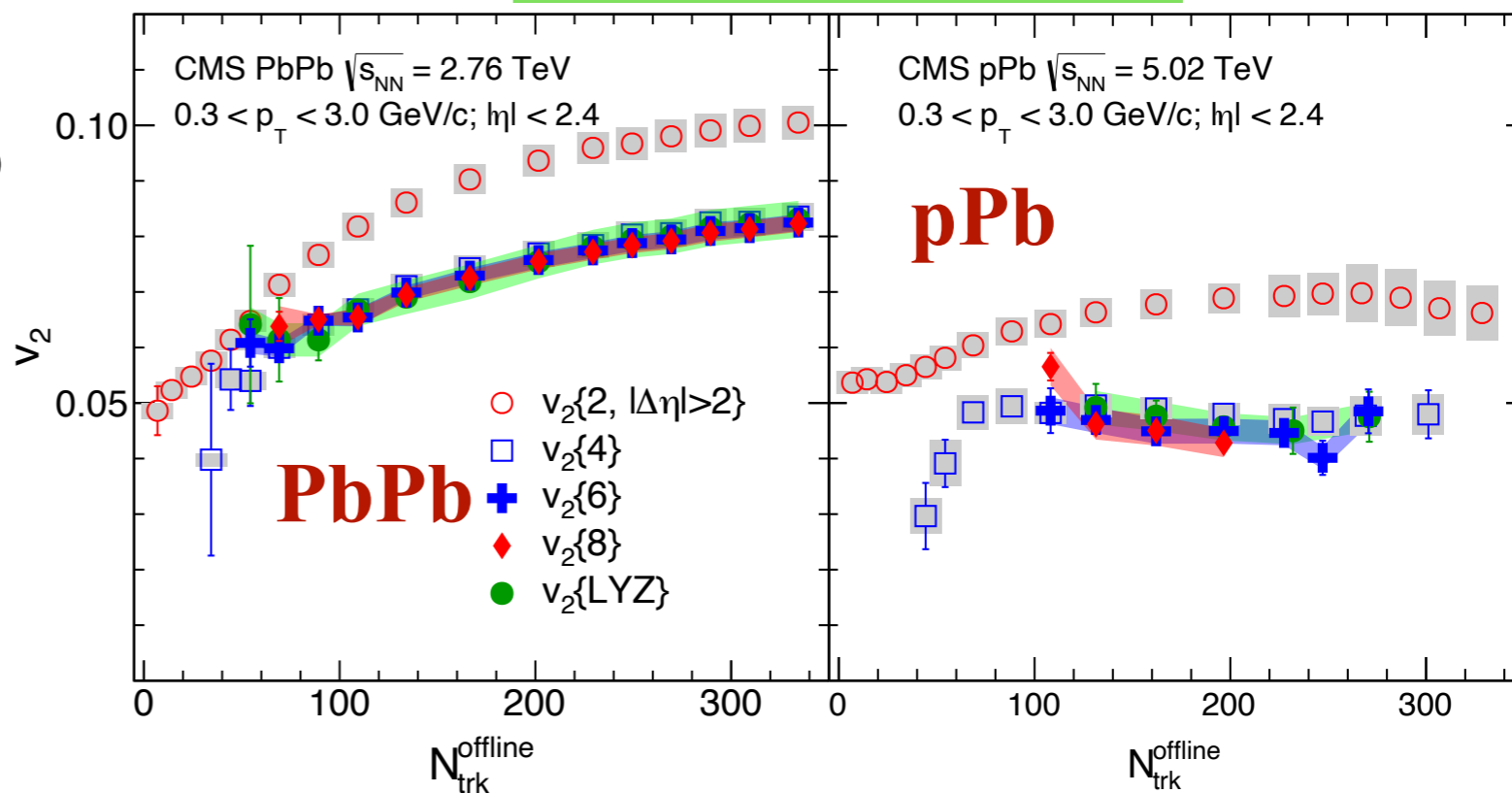


JHEP 07 (2011) 076

CMS PbPb 2.76 TeV 35-40%  
 $1 < p_T < 3$  GeV/c



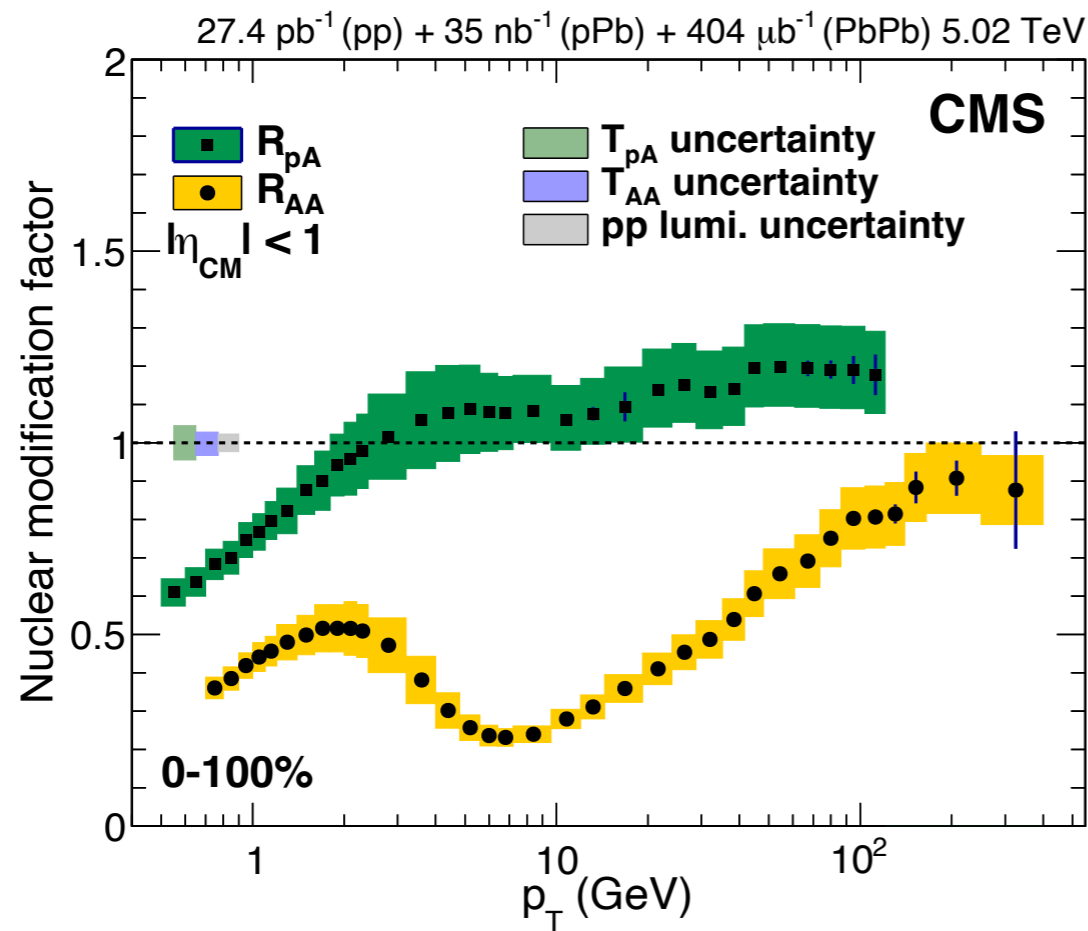
Phys. Rev. Lett. 115, 012301 (2015)



## ✿ Azimuthal Anisotropy ( $v_n$ ) at low $p_T$ ( $< 3$ GeV/c)

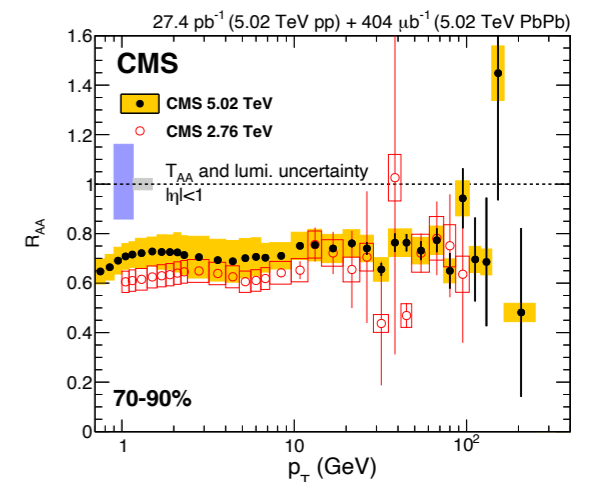
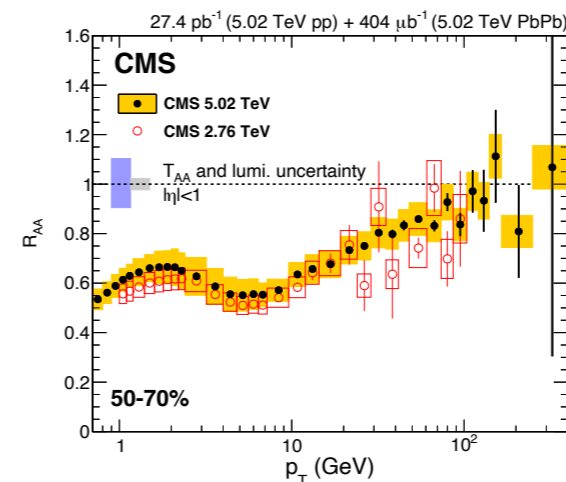
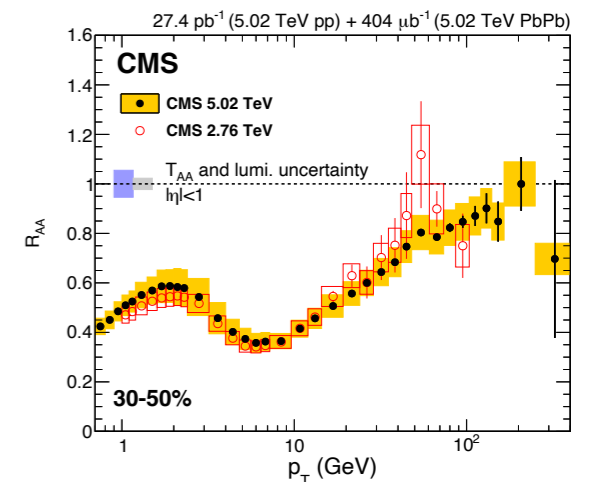
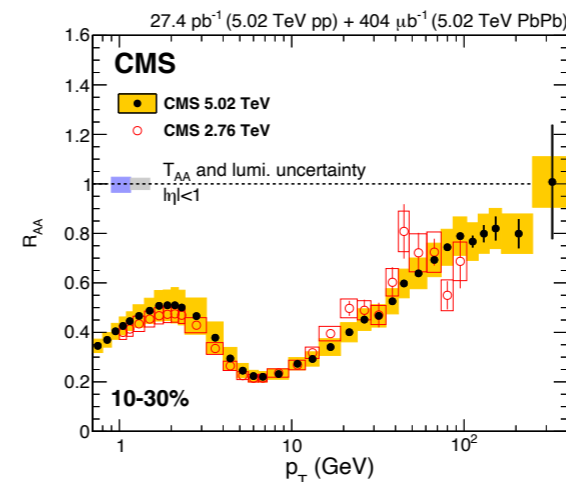
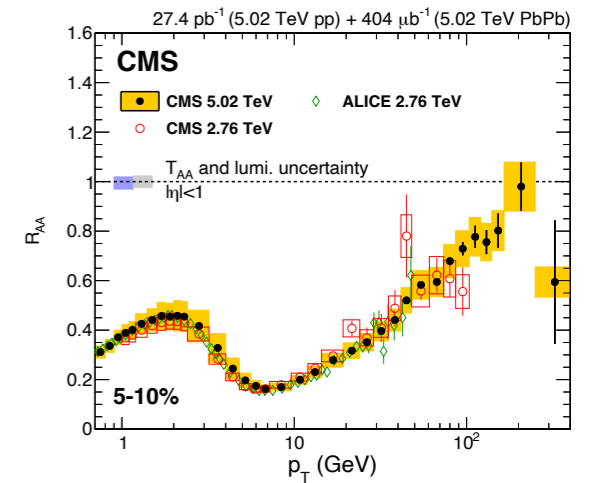
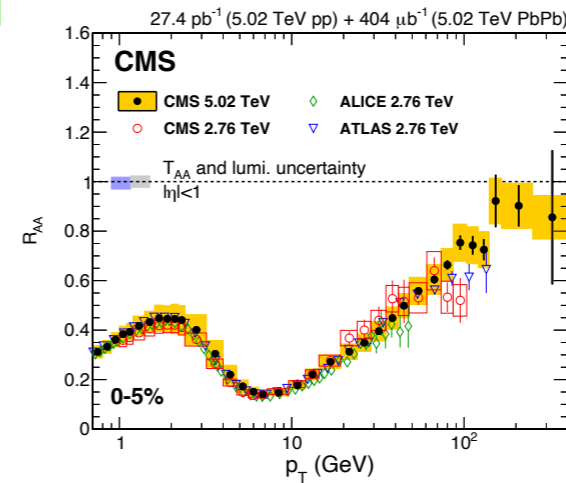
- ❖ Discovery of “Ridge” in pPb => sign of collectivity
- ❖ Geometry + Fluctuations
- ❖ Well described by hydrodynamics
- ❖  $v_2\{4\} \sim v_2\{6\} \sim v_2\{8\}$  from cumulant studies

JHEP 04 (2017) 039

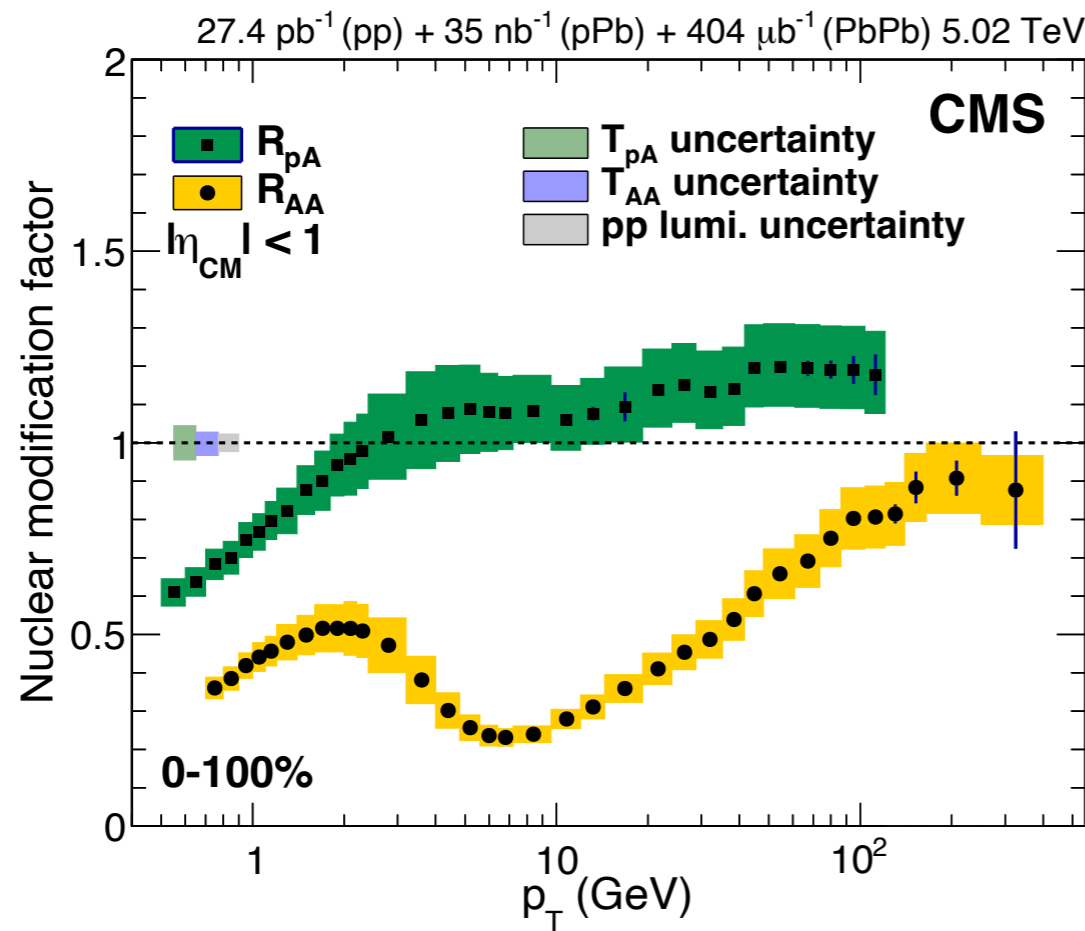


$$R_{AA} = \frac{N_{\text{particles}}^{A+A}}{N_{\text{particles}}^{p+p} \times N_{\text{coll}}}$$

- ❖  $R_{AA}$  shows max suppression in central bins in PbPb
- ❖ Weakening of both magnitude and  $p_T$  dependence in peripheral bins
- ❖ No suppression in 2-10 GeV region in **minimum bias** pPb
- ❖ Weak  $p_T$  dependence for  $p_T > 10$  GeV
- ❖ pPb: similar system size as peripheral PbPb but no suppression  
(Caution: Complications from centrality bias factors in pPb)

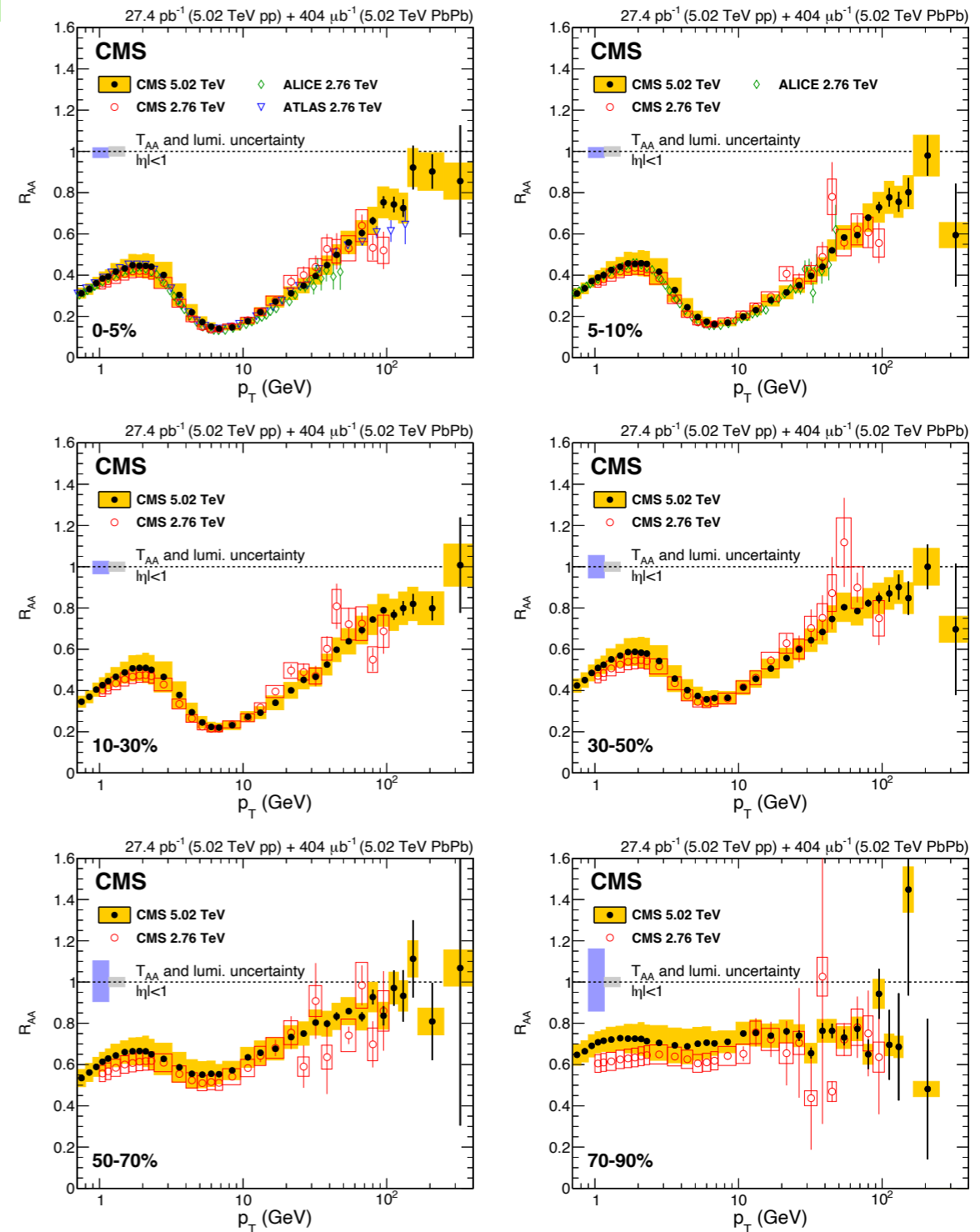


JHEP 04 (2017) 039

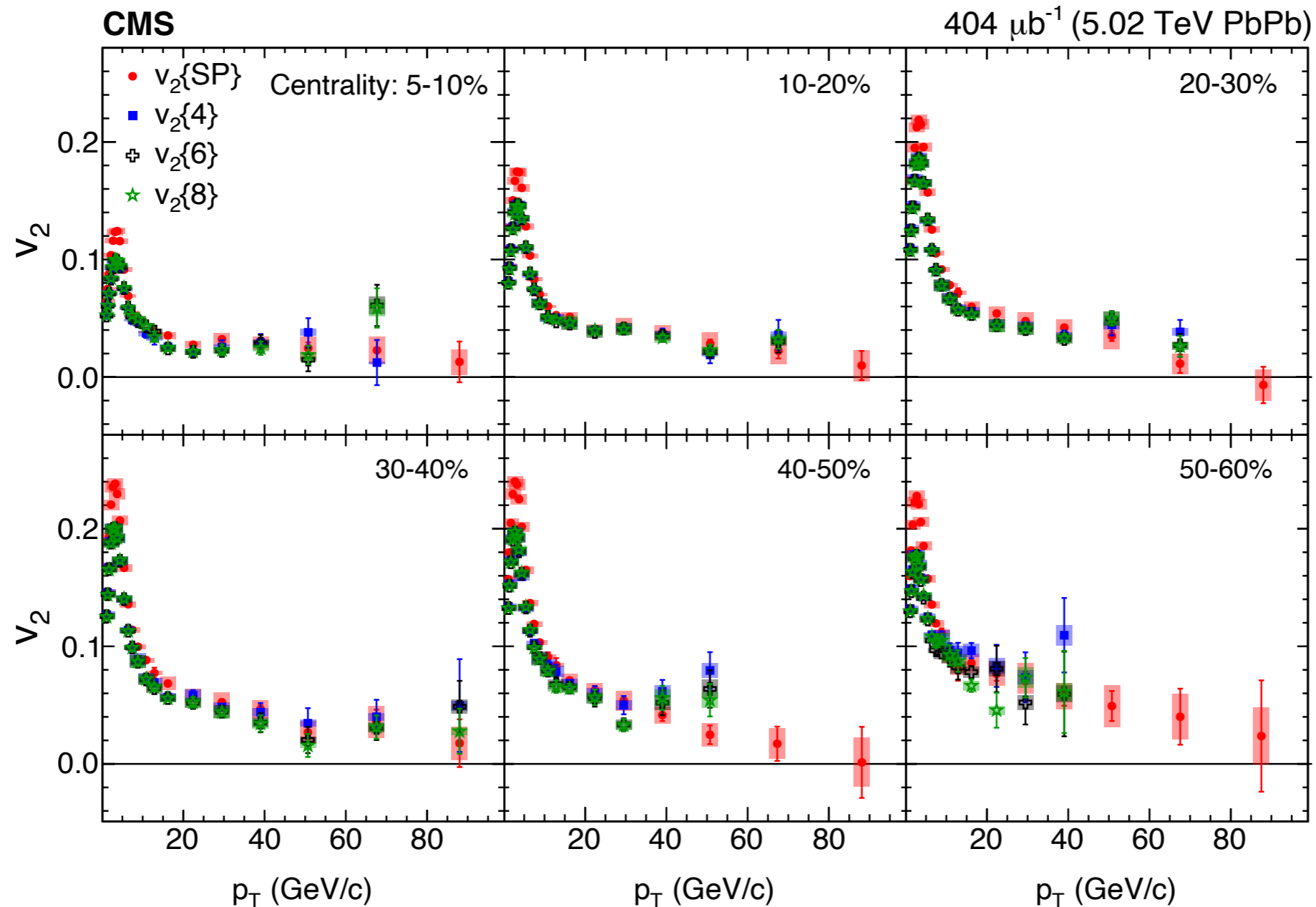


$$R_{AA} = \frac{N_{\text{particles}}^{A+A}}{N_{\text{particles}}^{p+p} \times N_{\text{coll}}}$$

- ❖  $R_{AA}$  shows max suppression in central bins in PbPb
- ❖ Weakening of both magnitude and  $p_T$  dependence in peripheral bins
- ❖ No suppression in 2-10 GeV region in **minimum bias** pPb
- ❖ Weak  $p_T$  dependence for  $p_T > 10$  GeV
- ❖ pPb: similar system size as peripheral PbPb but no suppression  
(Caution: Complications from centrality bias factors in pPb)

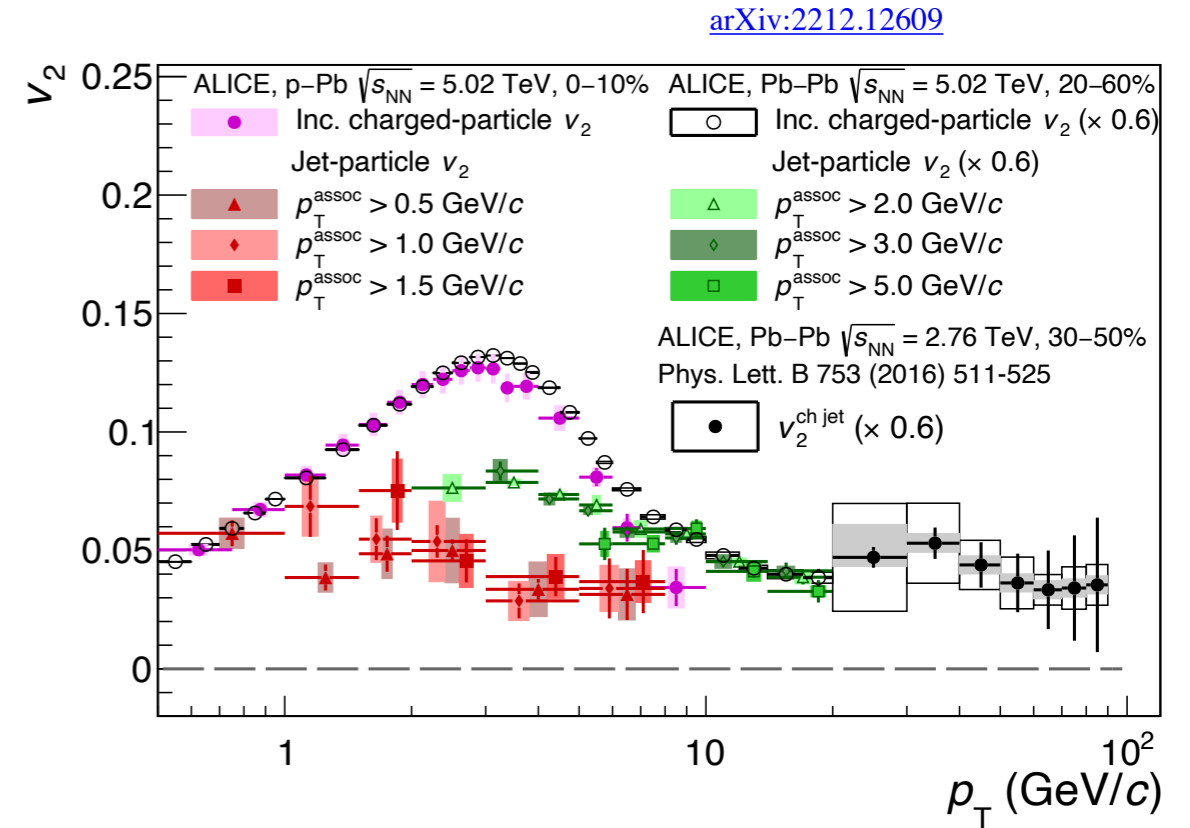
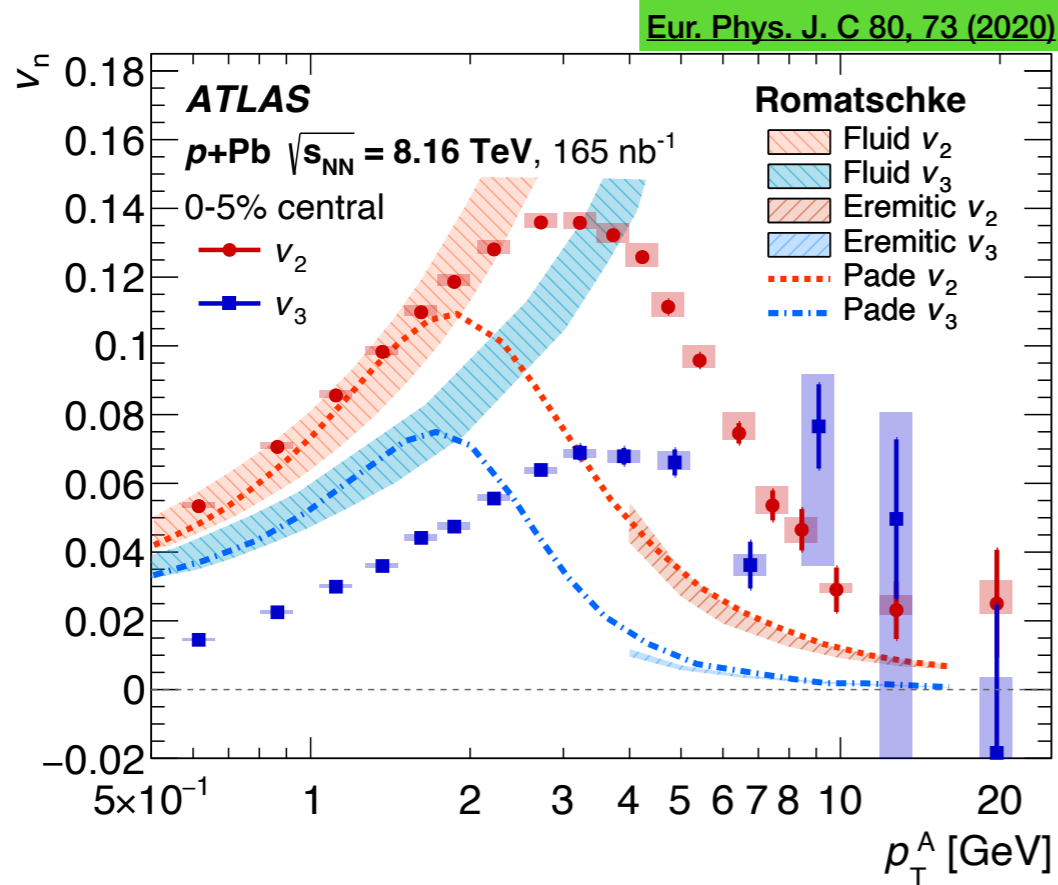


See Dener's talk on Jet Quenching in pPb

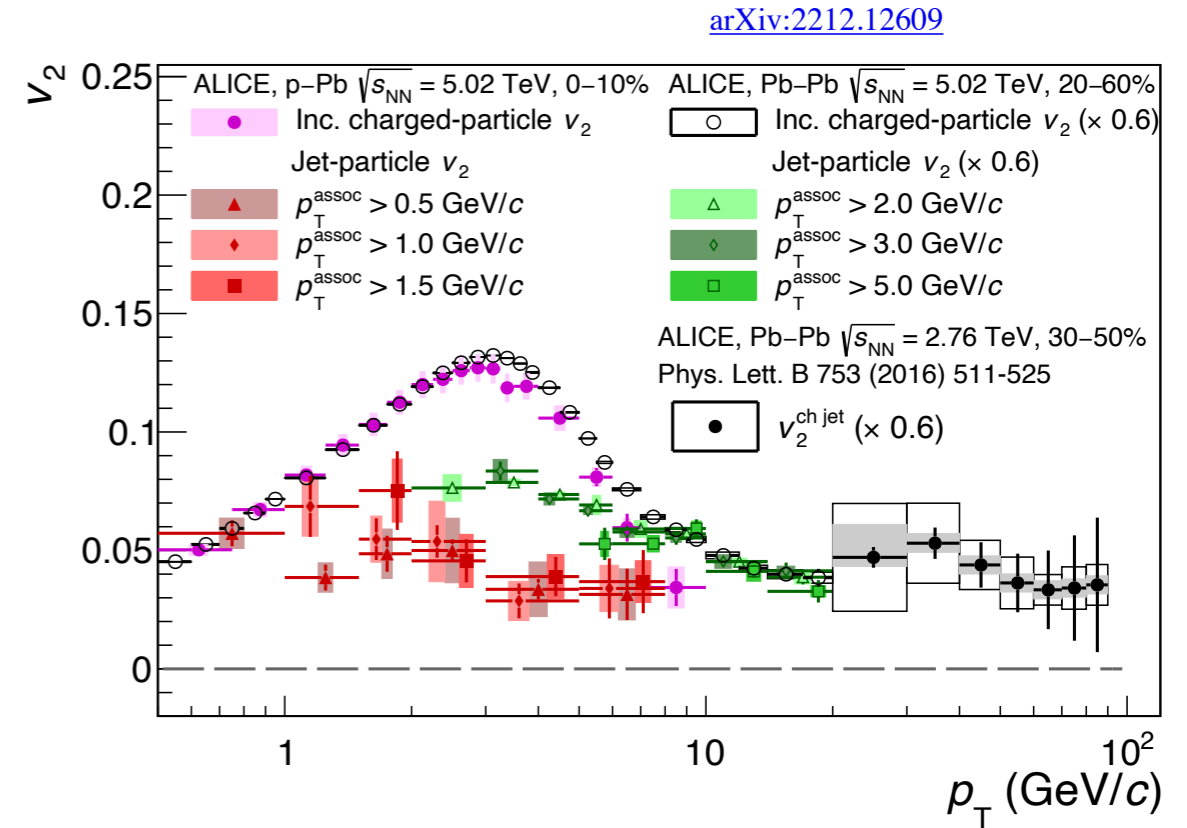
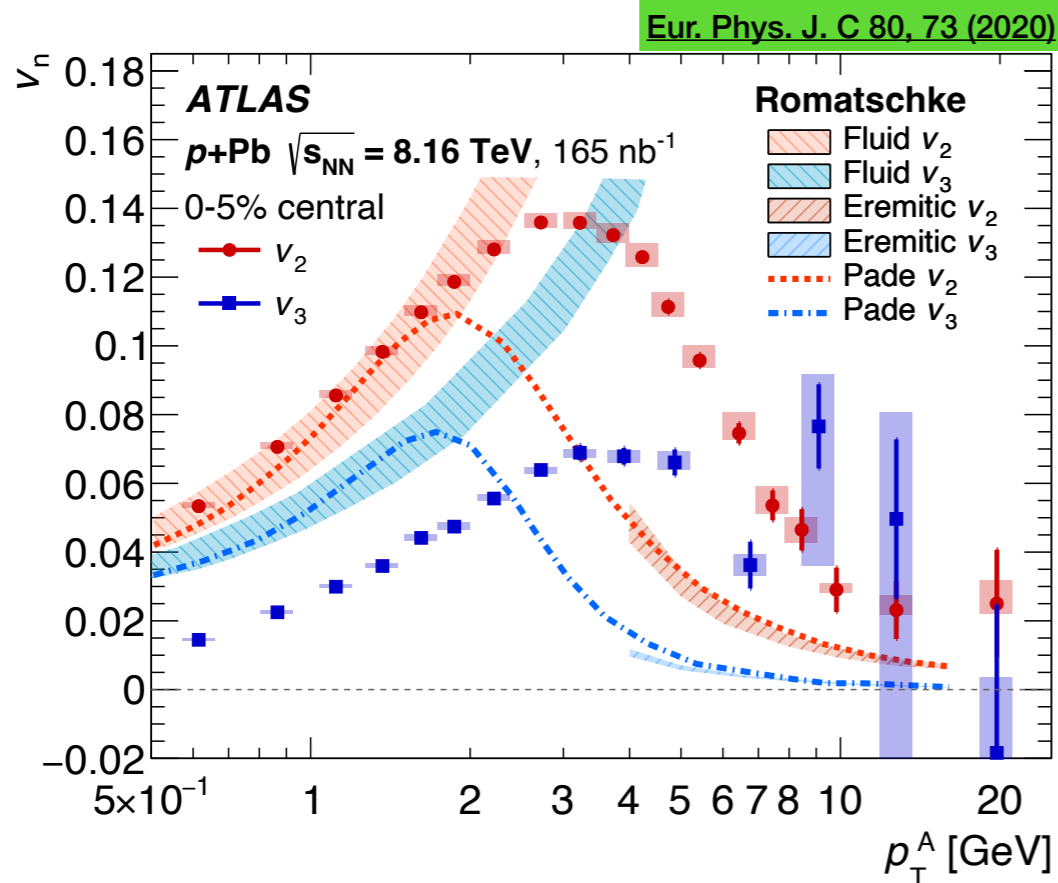


✳ **Azimuthal Anisotropy ( $v_n$ ) at high  $p_T$  ( $> 10$  GeV/c) in AA:**

- ❖ **Energy loss + Fluctuations, no hydrodynamics**
- ❖ **Sensitive to the path length of high  $p_T$  parton in QGP medium (Jet Quenching)**



- ❖ 2-particle correlation technique (nonflow contamination)
- ❖ Template fit method for nonflow subtraction
- ❖ Based on strong assumptions



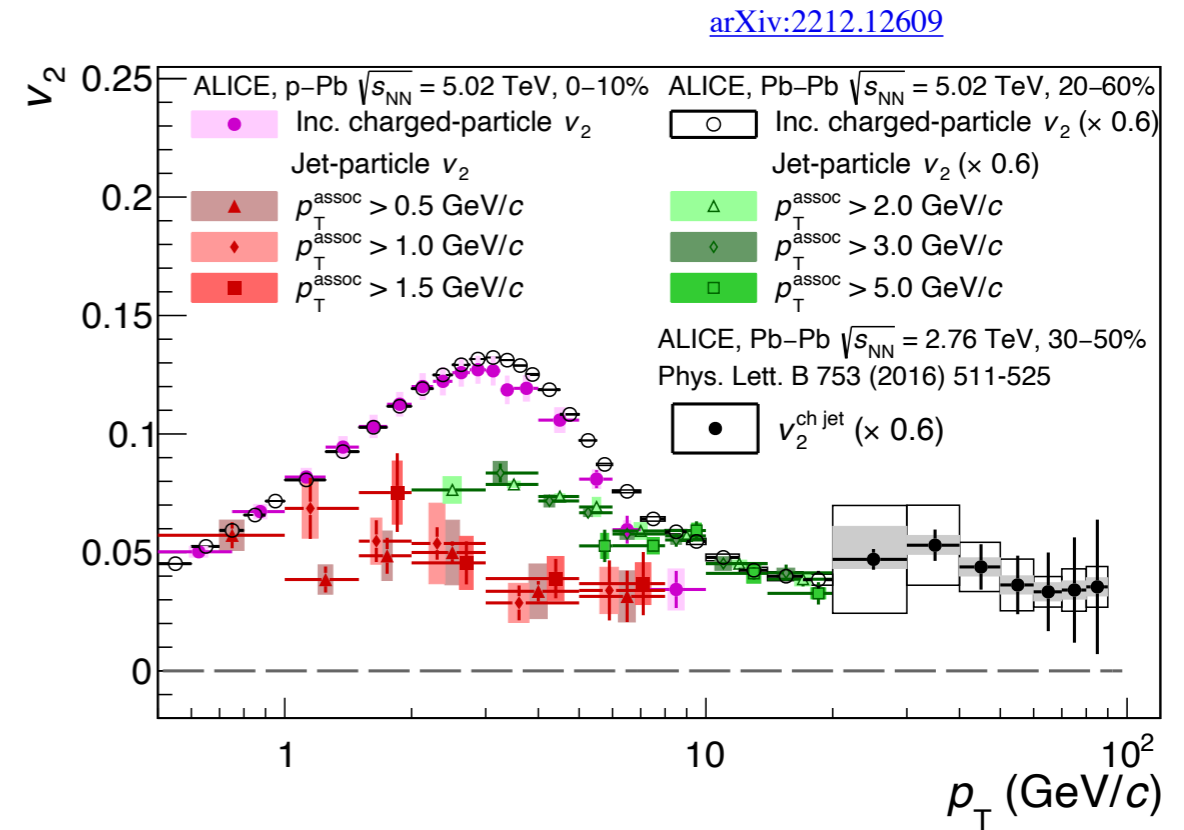
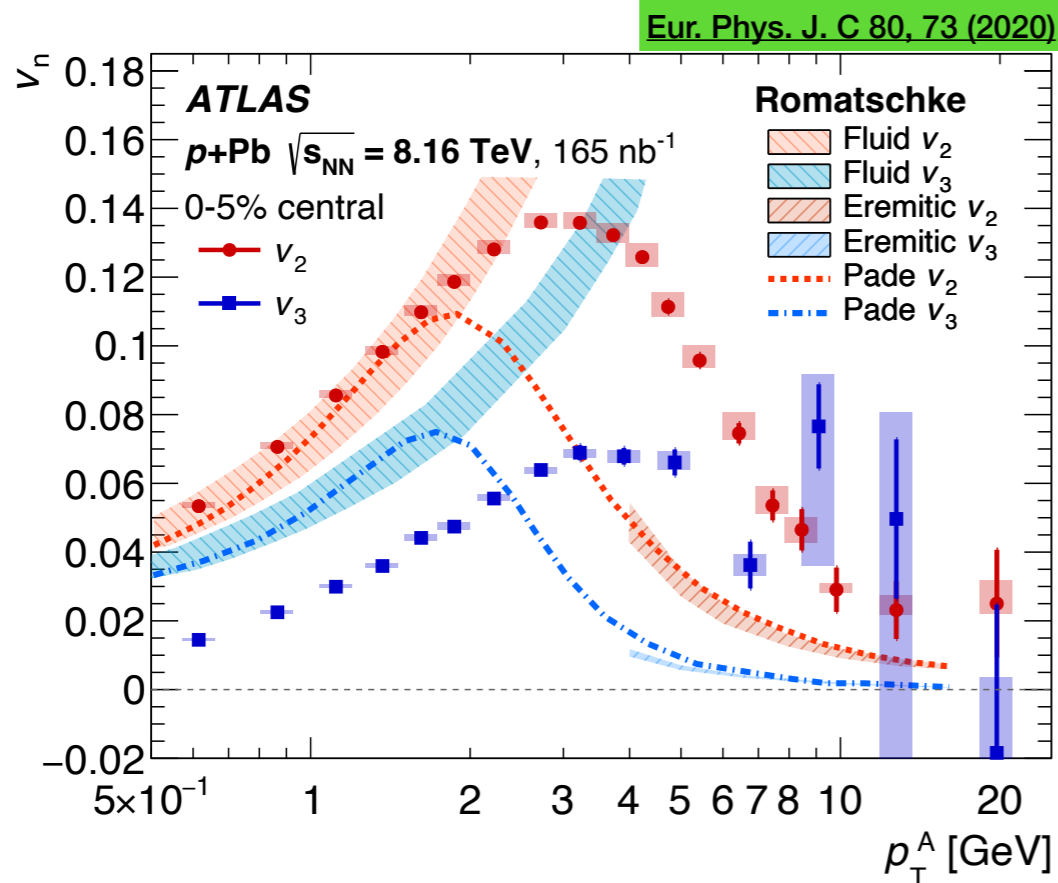
- ❖ 2-particle correlation technique (nonflow contamination)
- ❖ Template fit method for nonflow subtraction
- ❖ Based on strong assumptions

✳ **Open questions:**

- ❖ What could be the source of observed anisotropy at high  $p_T$  in pPb?
- ❖ How can there be a hydro medium that modifies the distribution of final-state hadrons yet has no impact on high  $p_T$  particle distribution?







- ❖ 2-particle correlation technique (nonflow contamination)
- ❖ Template fit method for nonflow subtraction
- ❖ Based on strong assumptions

✳ Open questions:

- ❖ What could be the source of observed anisotropy at high  $p_T$  in pPb?
- ❖ How can there be a hydro medium that modifies the distribution of final-state hadrons yet has no impact on high  $p_T$  particle distribution?



✳ Further study using Cumulants:

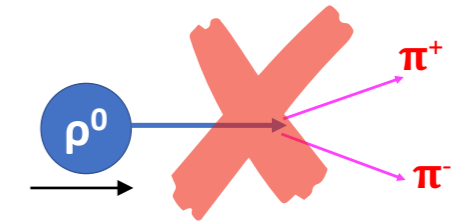
- ❖ Known to better mitigate nonflow
- ❖ **First** measurement of  $v_n$  using subevent cumulant at **high  $p_T$**  in high multiplicity pPb

## ✱ Cumulant method:

- ❖ Multiparticle correlation technique
- ❖ Non-flow suppression in a data-driven way

Phys.Rev.C83:044913,2011

$$c_n\{4\} = \langle\langle 4 \rangle\rangle - 2 \cdot \langle\langle 2 \rangle\rangle \langle\langle 2 \rangle\rangle$$



## ✱ Q-cumulant:

❖ Q-vector:  $Q_n \equiv \sum_{i=1}^M e^{in\phi_i}$

$\langle\langle 2 \rangle\rangle = \langle\langle e^{in(\phi_1 - \phi_2)} \rangle\rangle$ , and  $\langle\langle 4 \rangle\rangle = \langle\langle e^{in(\phi_1 + \phi_2 - \phi_3 - \phi_4)} \rangle\rangle$

Phys. Rev. C 89, 064904 (2014)

=> Cumulants :

•  $c_n\{2\} = \langle\langle 2 \rangle\rangle$       •  $c_n\{4\} = \langle\langle 4 \rangle\rangle - 2\langle\langle 2 \rangle\rangle \cdot \langle\langle 2 \rangle\rangle$

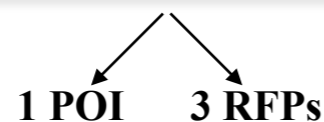
=> Flow :

•  $v_n\{2\} = \sqrt{c_n\{2\}}$       •  $v_n\{4\} = \sqrt[4]{-c_n\{4\}}$

=> Differential cumulant :  $d_n\{4\} = \langle\langle 4' \rangle\rangle - 2\langle\langle 2' \rangle\rangle \cdot \langle\langle 2 \rangle\rangle$

=> Differential Flow :

$$v'_n\{4\} = -\frac{d_n\{4\}}{(-c_n\{4\})^{3/4}}$$

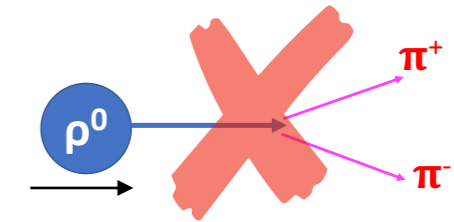


## ✱ Cumulant method:

- ❖ Multiparticle correlation technique
- ❖ Non-flow suppression in a data-driven way

$$c_n\{4\} = \langle\langle 4 \rangle\rangle - 2 \cdot \langle\langle 2 \rangle\rangle \langle\langle 2 \rangle\rangle$$

Phys.Rev.C83:044913,2011



## ✱ Q-cumulant:

❖ Q-vector:  $Q_n \equiv \sum_{i=1}^M e^{in\phi_i}$

$\langle\langle 2 \rangle\rangle = \langle\langle e^{in(\phi_1 - \phi_2)} \rangle\rangle$ , and  $\langle\langle 4 \rangle\rangle = \langle\langle e^{in(\phi_1 + \phi_2 - \phi_3 - \phi_4)} \rangle\rangle$

Phys. Rev. C 89, 064904 (2014)

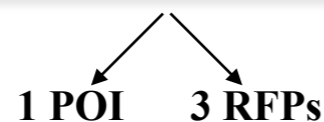
=> Cumulants :

•  $c_n\{2\} = \langle\langle 2 \rangle\rangle$       •  $c_n\{4\} = \langle\langle 4 \rangle\rangle - 2\langle\langle 2 \rangle\rangle \cdot \langle\langle 2 \rangle\rangle$

=> Flow :

•  $v_n\{2\} = \sqrt{c_n\{2\}}$       •  $v_n\{4\} = \sqrt[4]{-c_n\{4\}}$

=> Differential cumulant :  $d_n\{4\} = \langle\langle 4' \rangle\rangle - 2\langle\langle 2' \rangle\rangle \cdot \langle\langle 2 \rangle\rangle$



=> Differential Flow :

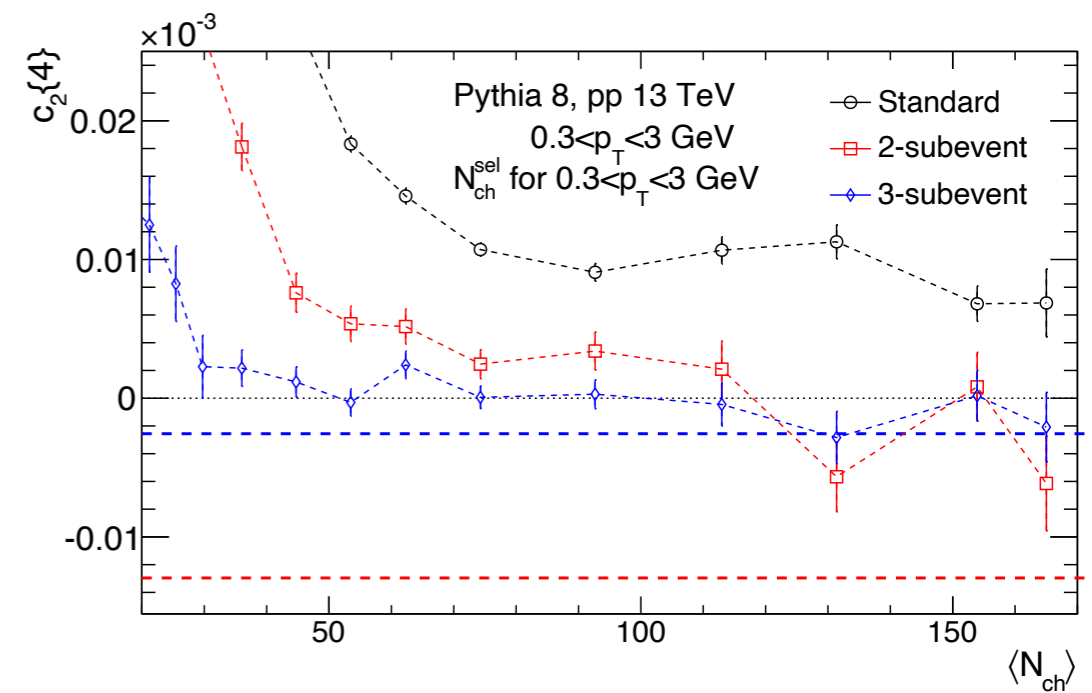
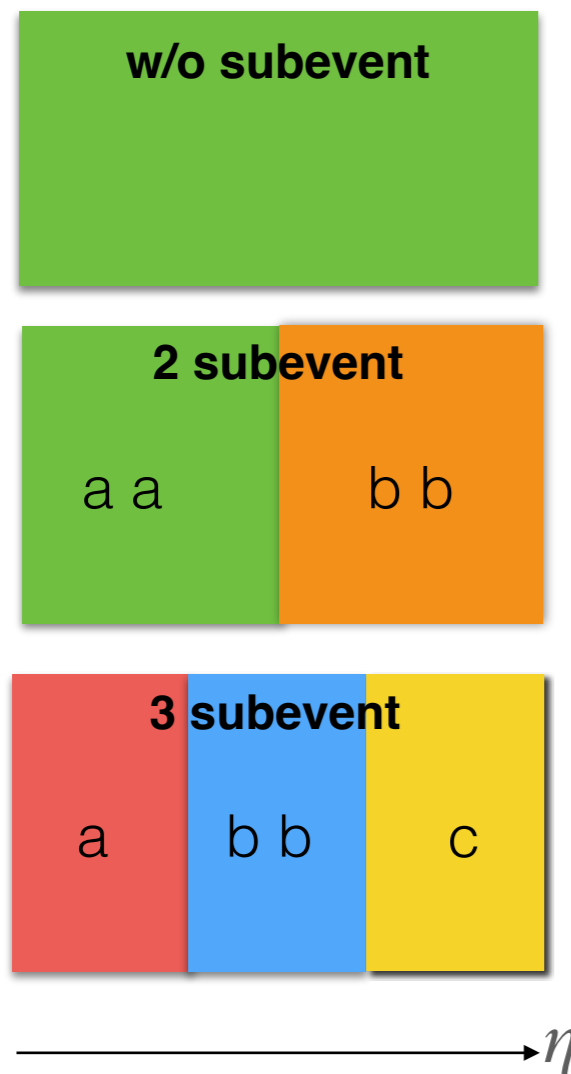
$$v'_n\{4\} = -\frac{d_n\{4\}}{(-c_n\{4\})^{3/4}}$$

Final observable

## Subevent technique:

In order to further suppress few-particle correlations and to explore possible collective correlation signals, we are using subevent cumulant techniques to require rapidity gaps among the particles

- 2 subevent can reduce non-flow contribution from within the Jets
- 3 and 4 subevents can remove back to back contribution

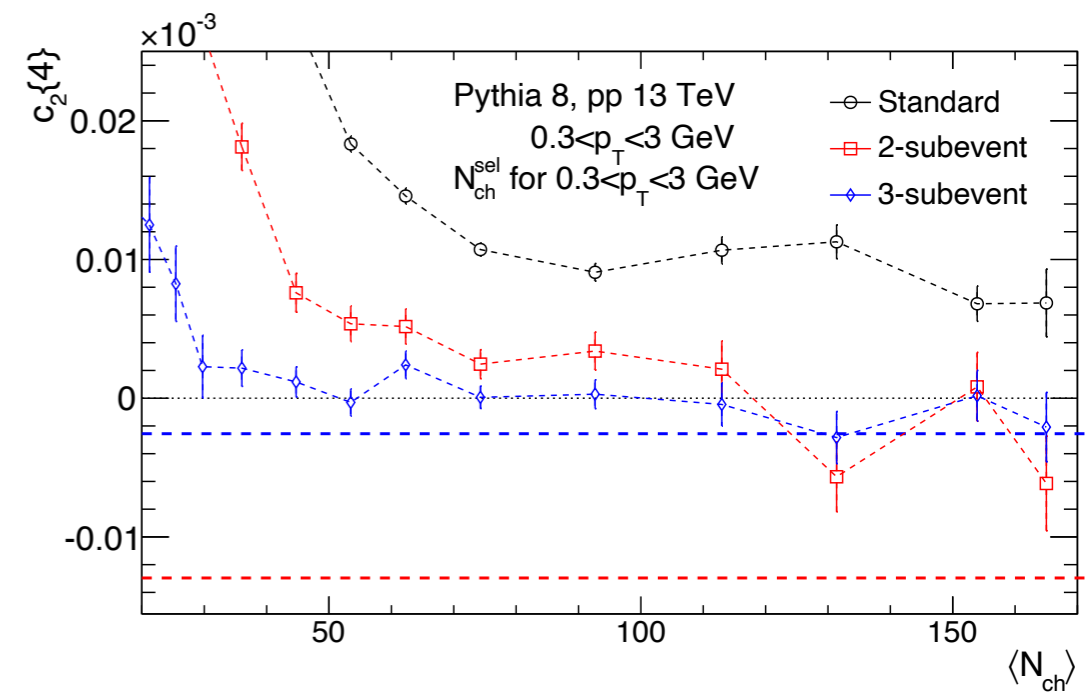
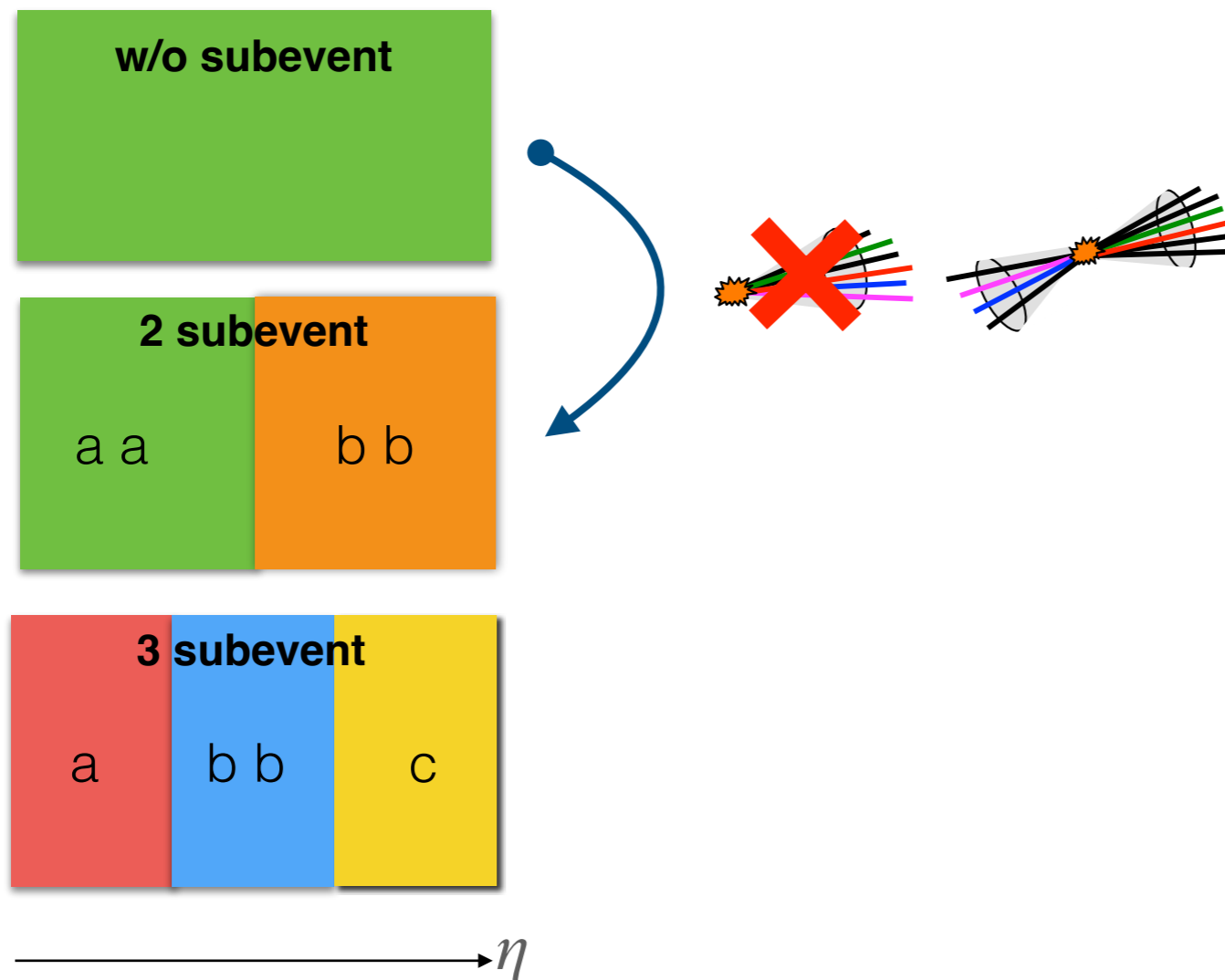


Phys. Rev. C 96, 034906 (2017)

## Subevent technique:

In order to further suppress few-particle correlations and to explore possible collective correlation signals, we are using subevent cumulant techniques to require rapidity gaps among the particles

- 2 subevent can reduce non-flow contribution from within the Jets
- 3 and 4 subevents can remove back to back contribution

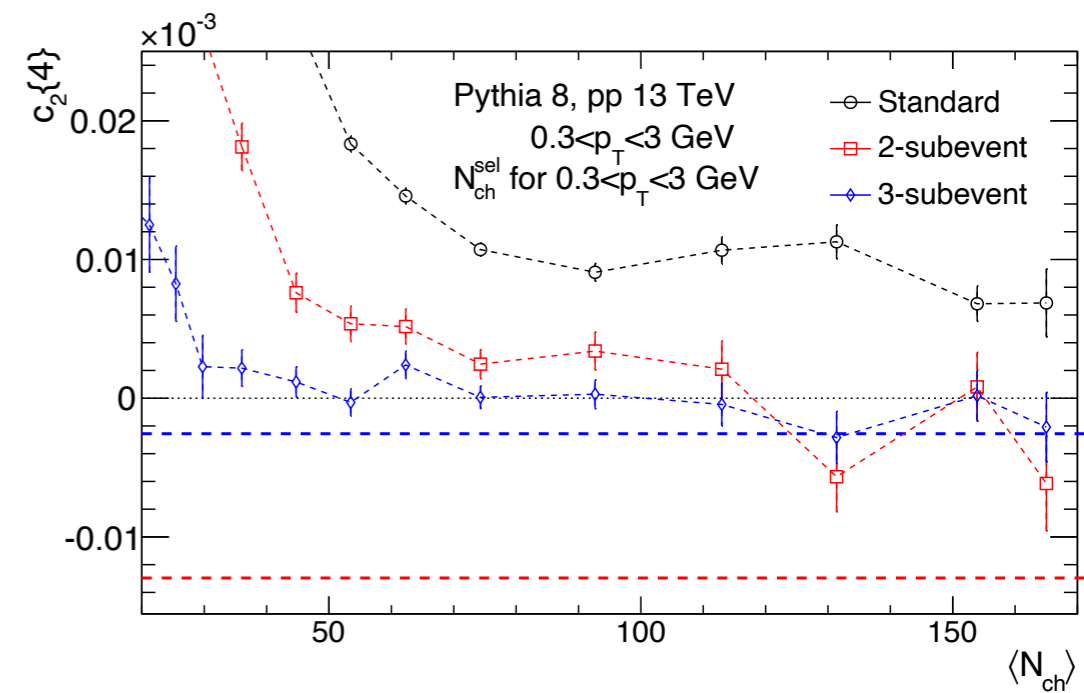
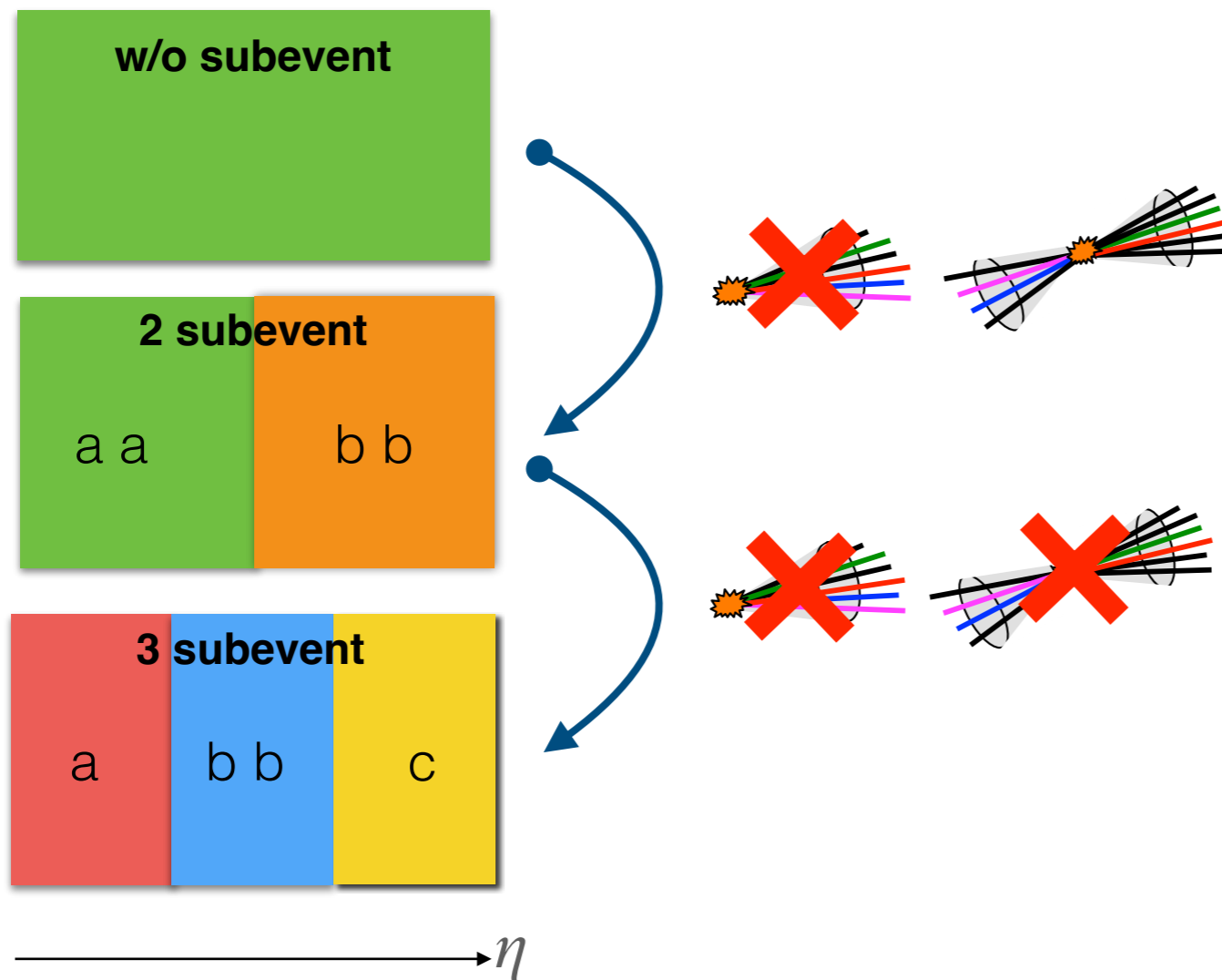


Phys. Rev. C 96, 034906 (2017)

## Subevent technique:

In order to further suppress few-particle correlations and to explore possible collective correlation signals, we are using subevent cumulant techniques to require rapidity gaps among the particles

- 2 subevent can reduce non-flow contribution from within the Jets
- 3 and 4 subevents can remove back to back contribution

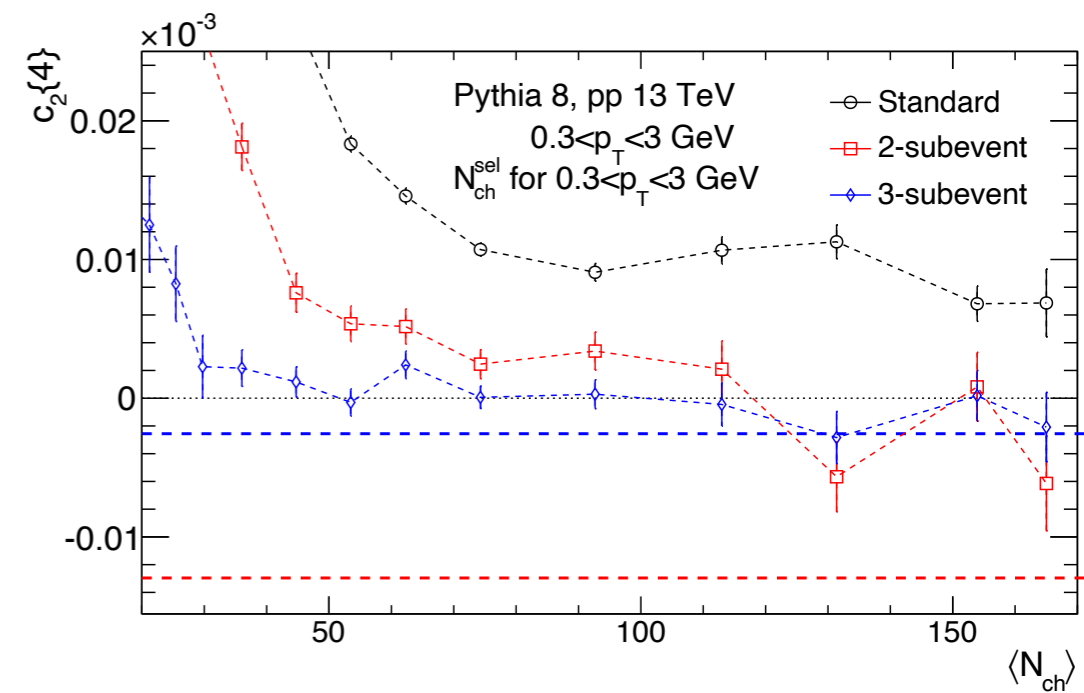
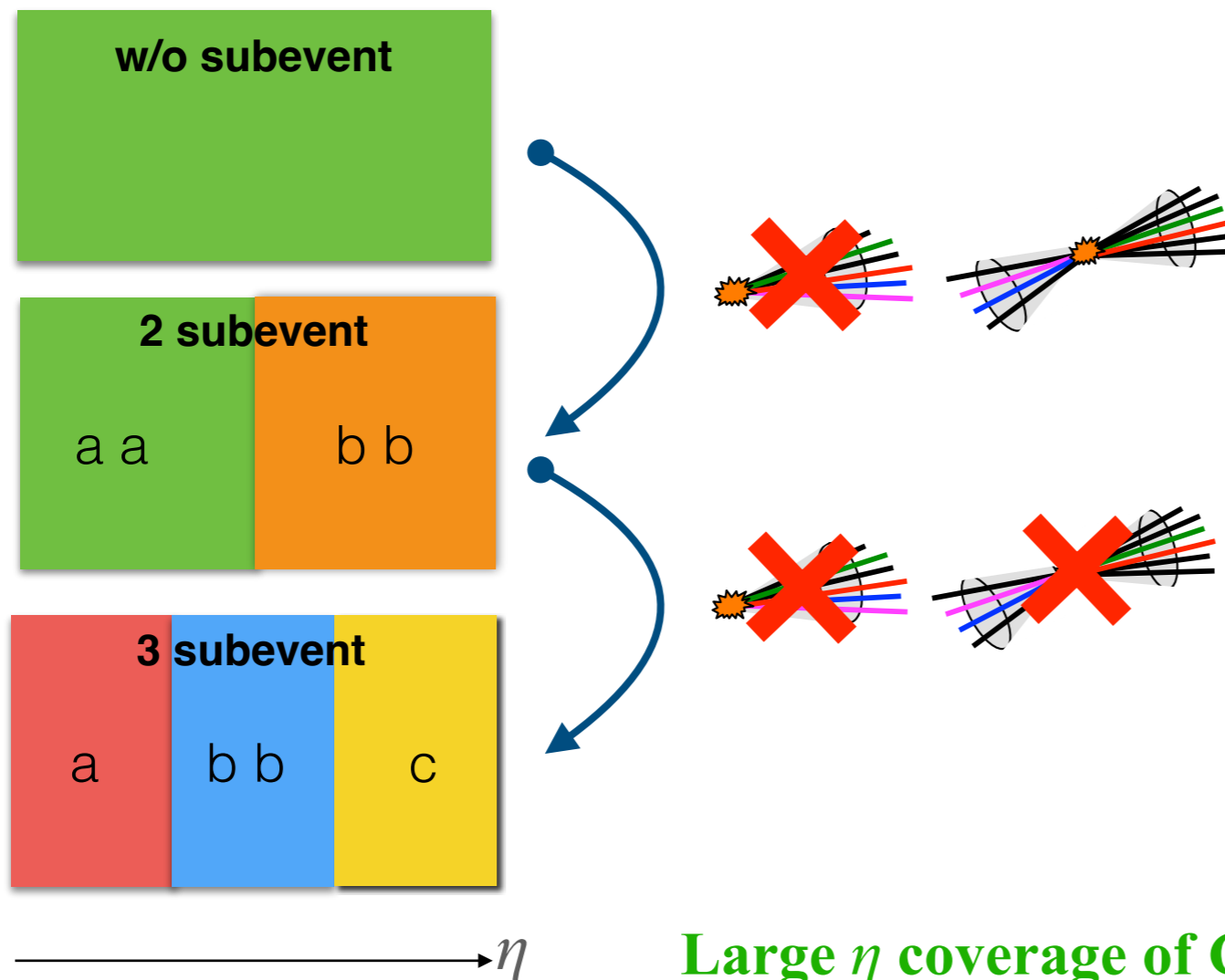


Phys. Rev. C 96, 034906 (2017)

## Subevent technique:

In order to further suppress few-particle correlations and to explore possible collective correlation signals, we are using subevent cumulant techniques to require rapidity gaps among the particles

- 2 subevent can reduce non-flow contribution from within the Jets
- 3 and 4 subevents can remove back to back contribution



Phys. Rev. C 96, 034906 (2017)

Large  $\eta$  coverage of CMS: enough statistics

# CMS DETECTOR

Total weight : 14,000 tonnes  
 Overall diameter : 15.0 m  
 Overall length : 28.7 m  
 Magnetic field : 3.8 T

STEEL RETURN YOKE  
 12,500 tonnes

SILICON TRACKERS  
 Pixel (100x150  $\mu\text{m}$ )  $\sim 1\text{m}^2 \sim 66\text{M}$  channels  
 Microstrips (80x180  $\mu\text{m}$ )  $\sim 200\text{m}^2 \sim 9.6\text{M}$  channels

SUPERCONDUCTING SOLENOID  
 Niobium titanium coil carrying  $\sim 18,000\text{A}$

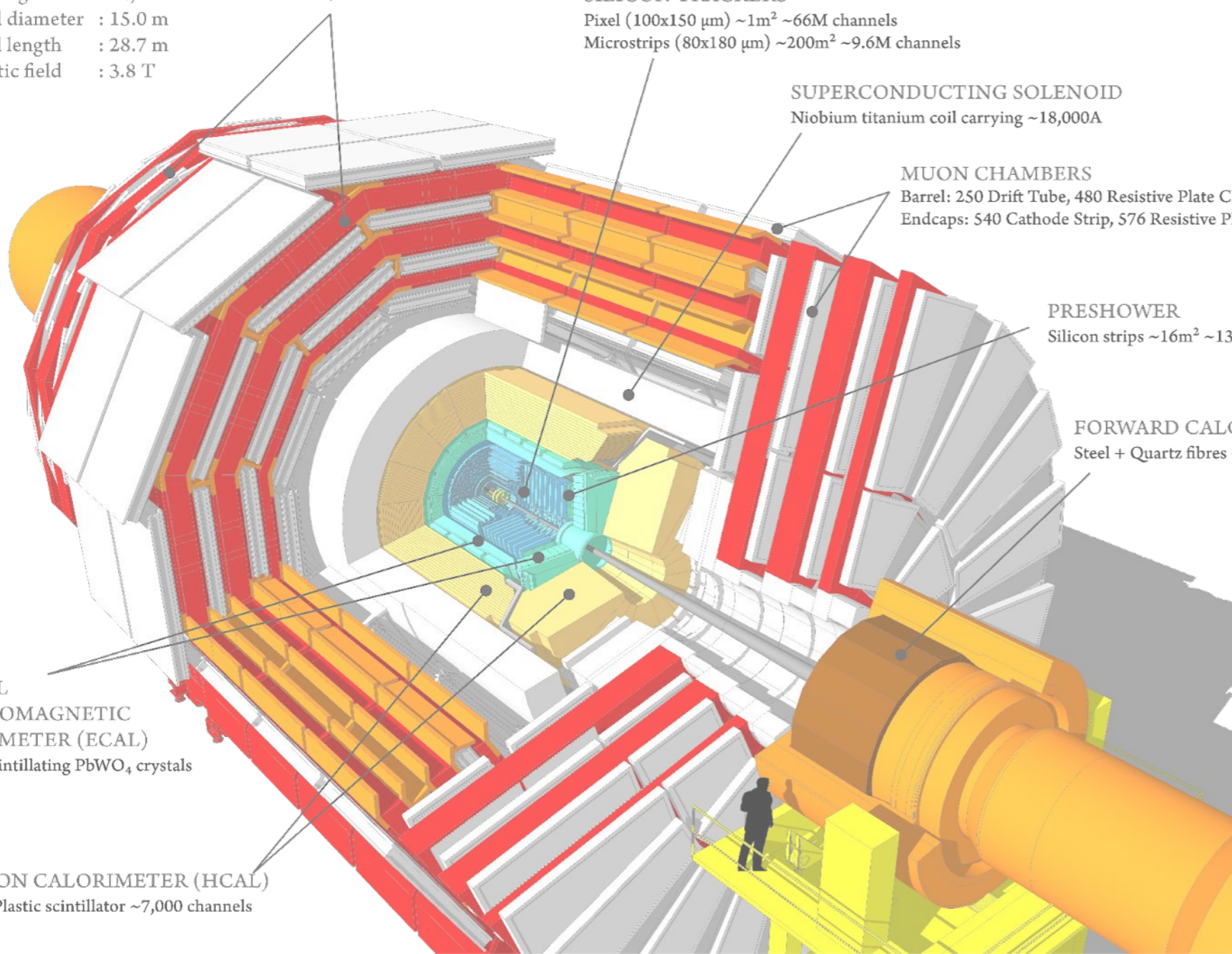
MUON CHAMBERS  
 Barrel: 250 Drift Tube, 480 Resistive Plate Chambers  
 Endcaps: 540 Cathode Strip, 576 Resistive Plate Chambers

PRESHOWER  
 Silicon strips  $\sim 16\text{m}^2 \sim 137,000$  channels

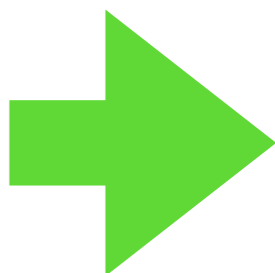
FORWARD CALORIMETER  
 Steel + Quartz fibres  $\sim 2,000$  Channels

CRYSTAL ELECTROMAGNETIC CALORIMETER (ECAL)  
 $\sim 76,000$  scintillating  $\text{PbWO}_4$  crystals

HADRON CALORIMETER (HCAL)  
 Brass + Plastic scintillator  $\sim 7,000$  channels



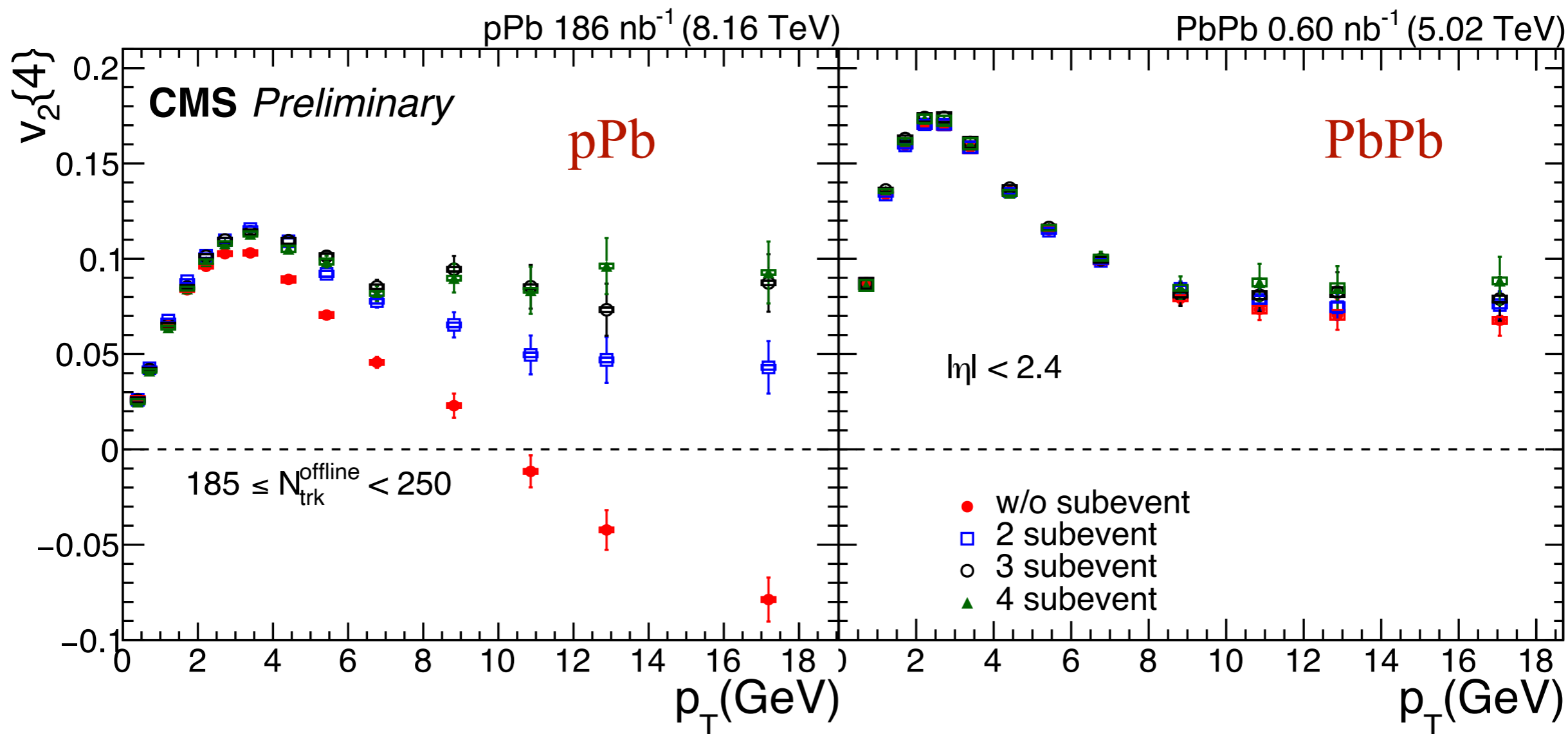
# Results





✱  $v_2\{4\}$  in  $185 \leq N_{trk}^{offline} < 250$  as a function of  $p_T$

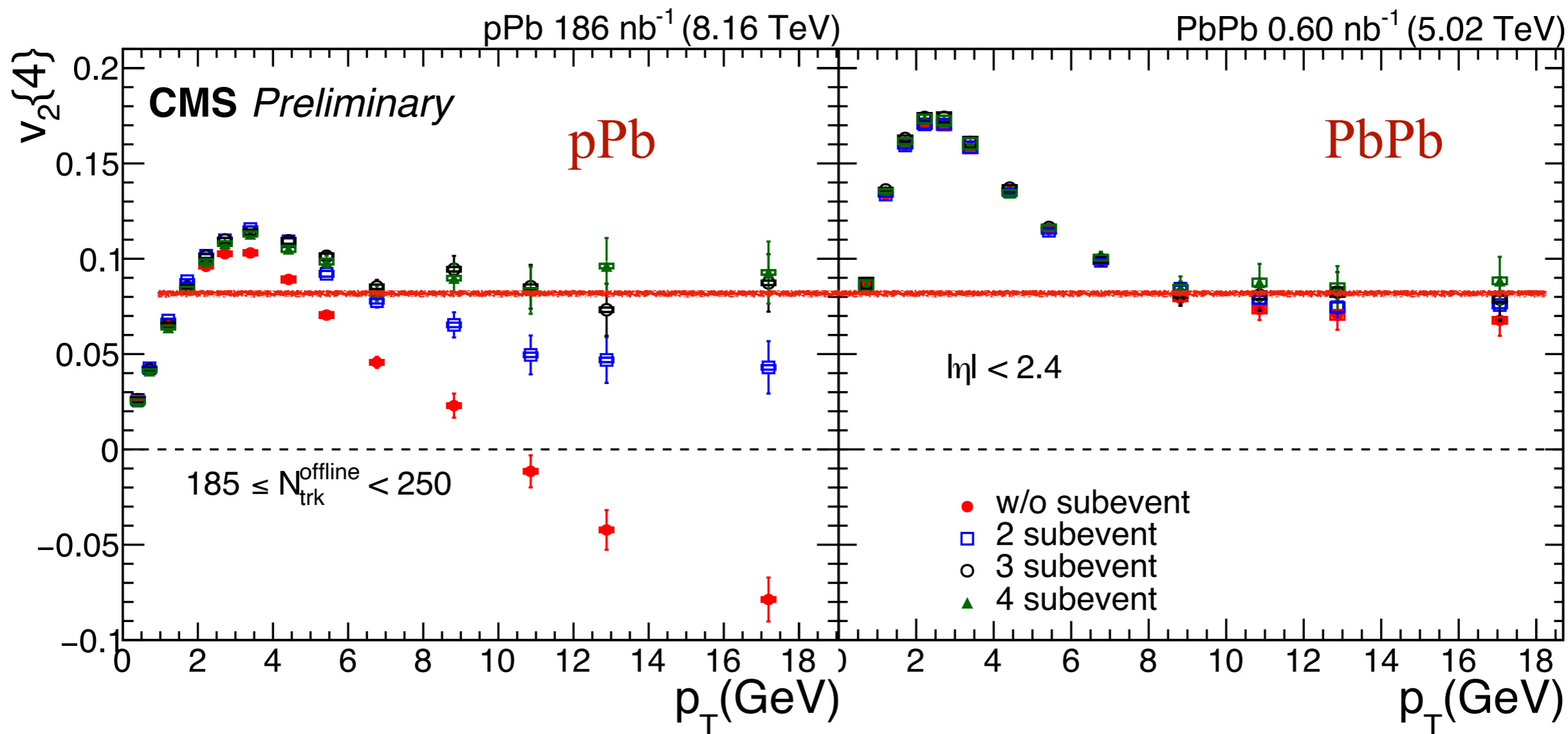
CMS-PAS-HIN-23-002



- At low  $p_T$ , PbPb has larger  $v_2\{4\}$  than pPb
- At high  $p_T$ , similar magnitude and similar trend of subevent  $v_2\{4\}$

✱  $v_2\{4\}$  in  $185 \leq N_{trk}^{offline} < 250$  as a function of  $p_T$

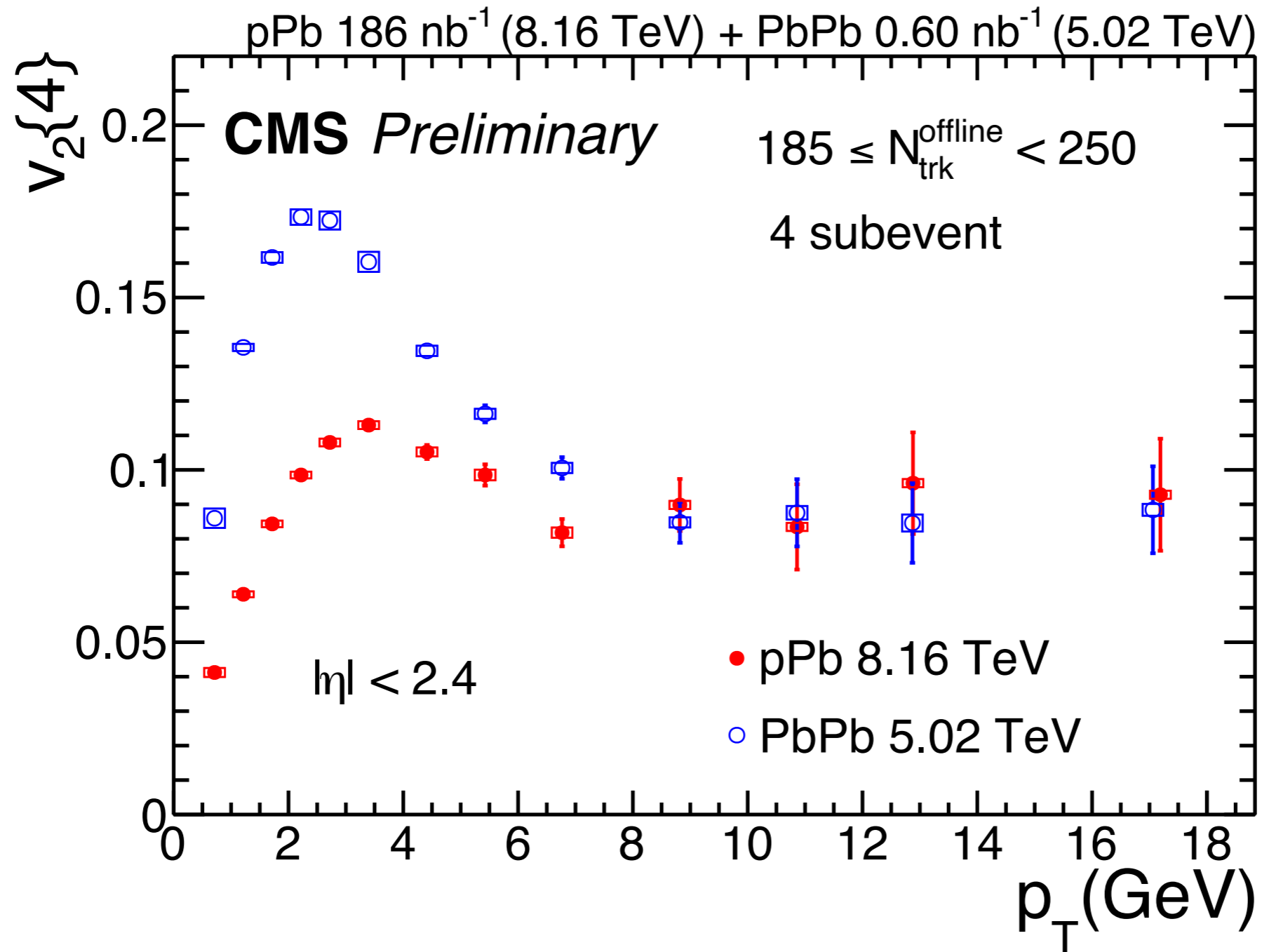
CMS-PAS-HIN-23-002



- At low  $p_T$ , PbPb has larger  $v_2\{4\}$  than pPb
- At high  $p_T$ , similar magnitude and similar trend of subevent  $v_2\{4\}$

✱ 4 subevent  $v_2\{4\}$  in  $185 \leq (N_{trk}^{offline}) < 250$

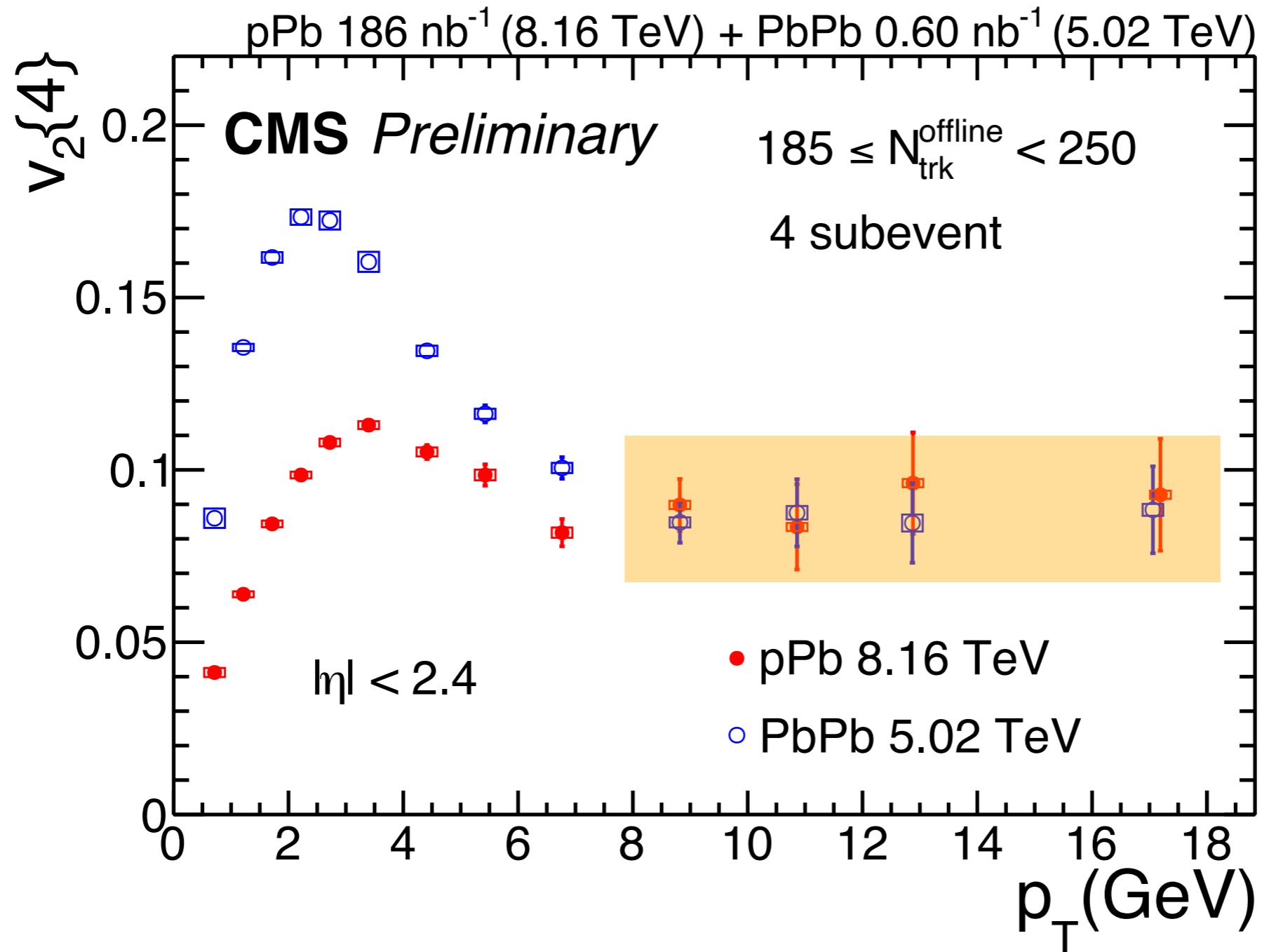
CMS-PAS-HIN-23-002



- At low  $p_T$ , PbPb has larger  $v_2\{4\}$  than pPb
- At high  $p_T$ , similar magnitude and similar trend of 4 subevent values

✱ **4 subevent  $v_2\{4\}$  in  $185 \leq (N_{trk}^{offline}) < 250$**

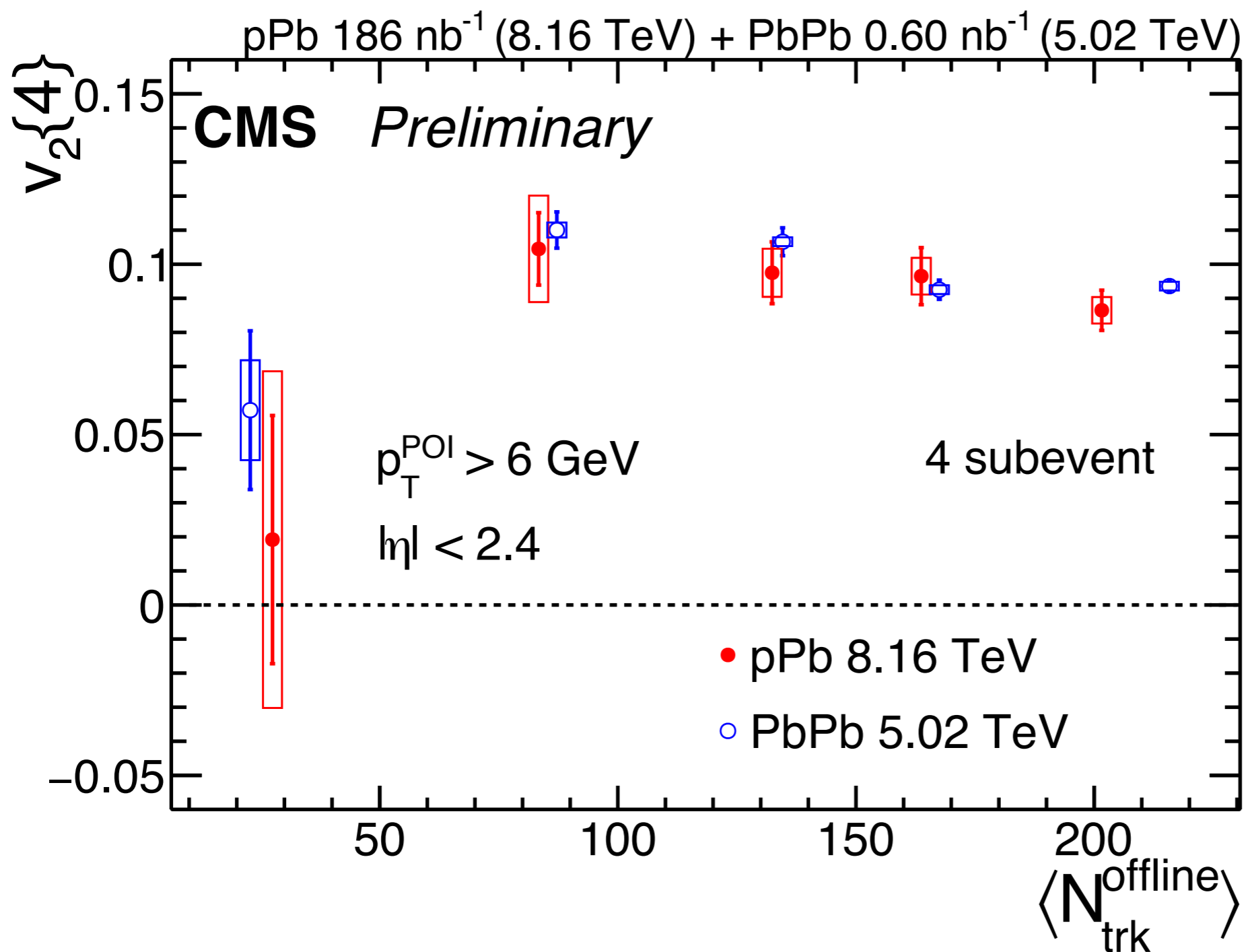
**CMS-PAS-HIN-23-002**



- At low  $p_T$ , PbPb has larger  $v_2\{4\}$  than pPb
- At high  $p_T$ , similar magnitude and similar trend of 4 subevent values

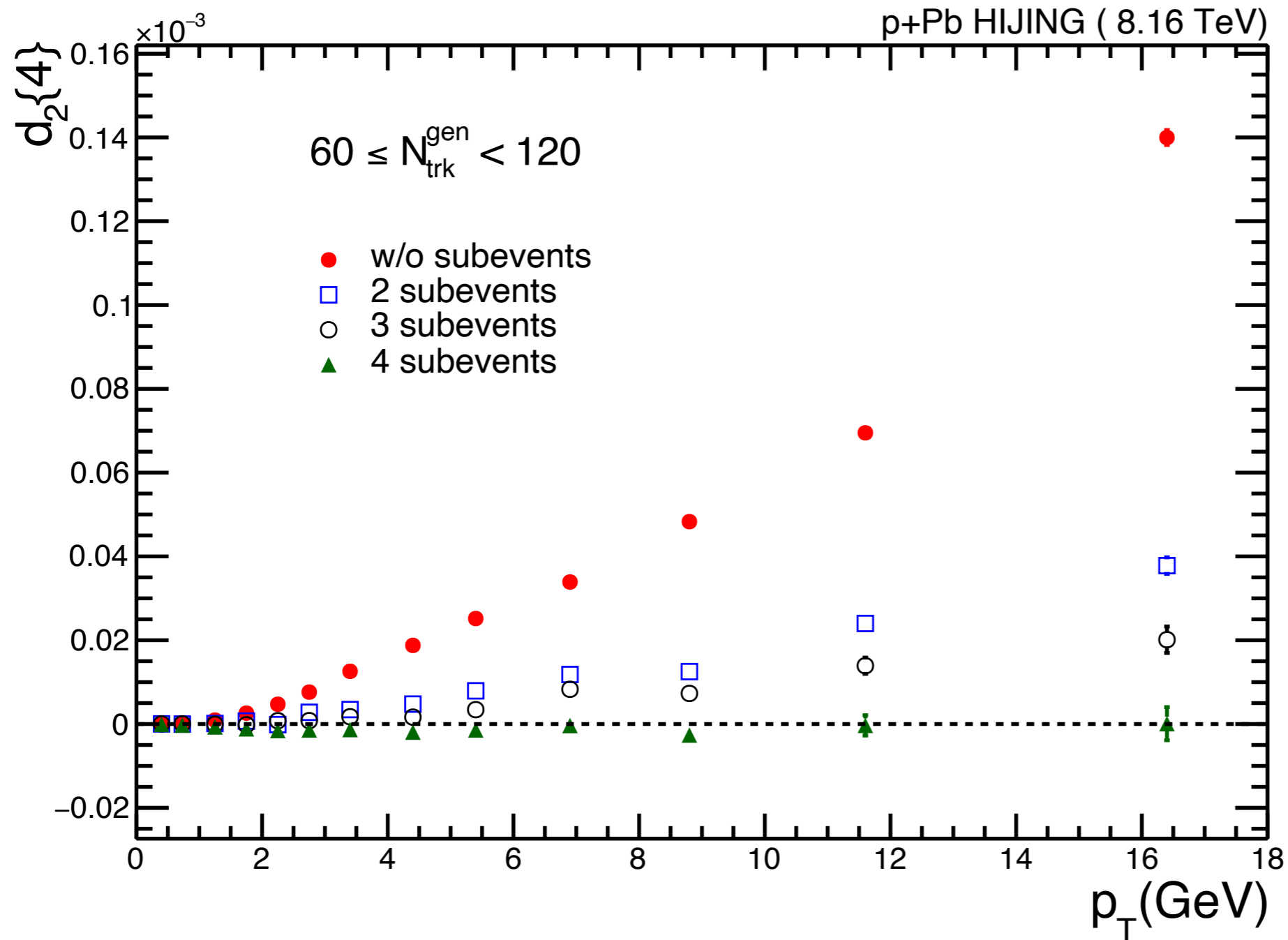
✱  $v_2\{4\}$  in different  $N_{trk}^{offline}$  bins with  $p_T^{POI} > 6$  GeV

CMS-PAS-HIN-23-002



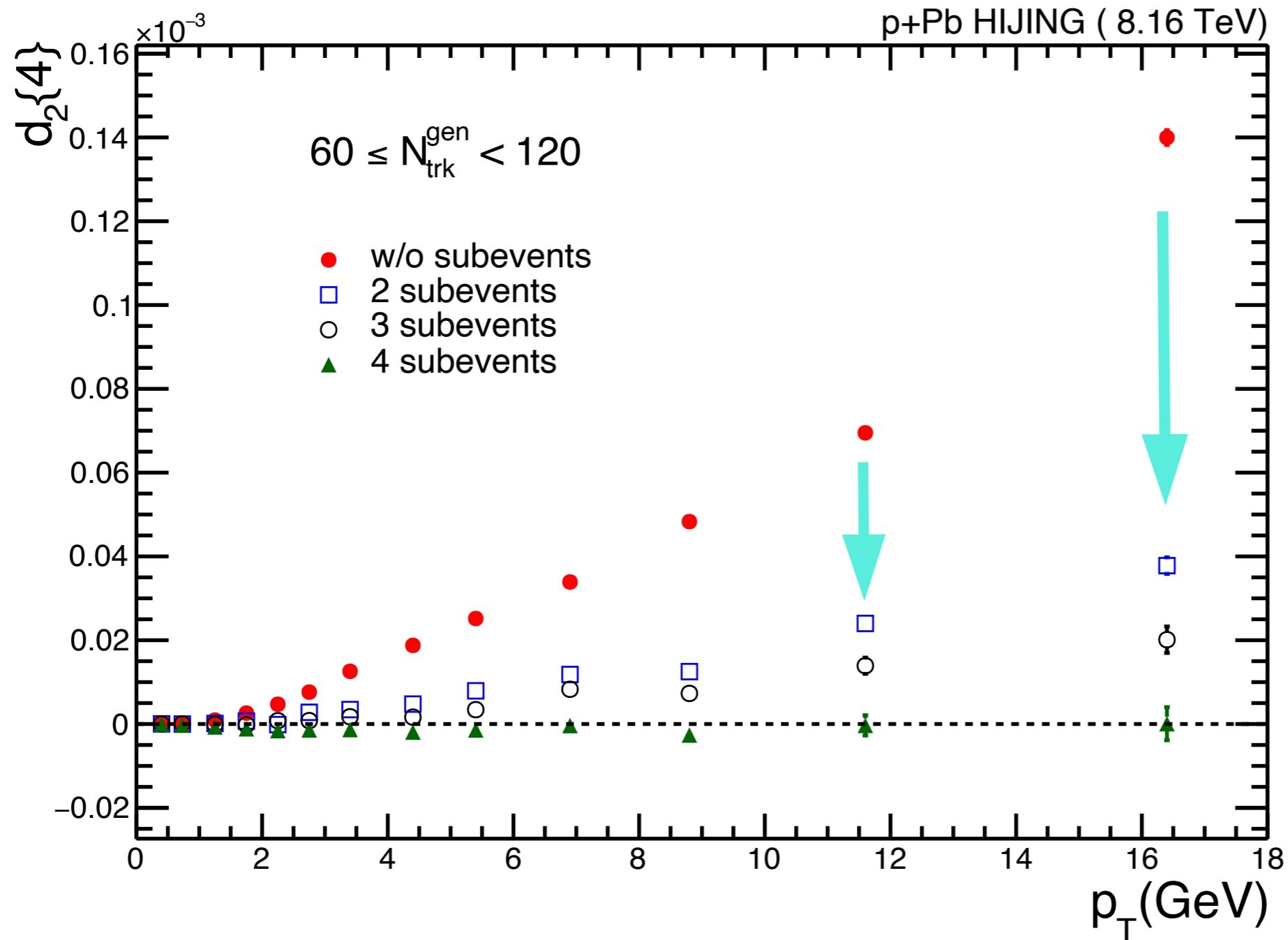
- Similar magnitude and trend for both PbPb and pPb when  $p_T^{POI} > 6$  GeV across all multiplicity bins

✱  $d_2\{4\}$  in **HIJING** in  $60 \leq (N_{trk}^{gen}) < 120$



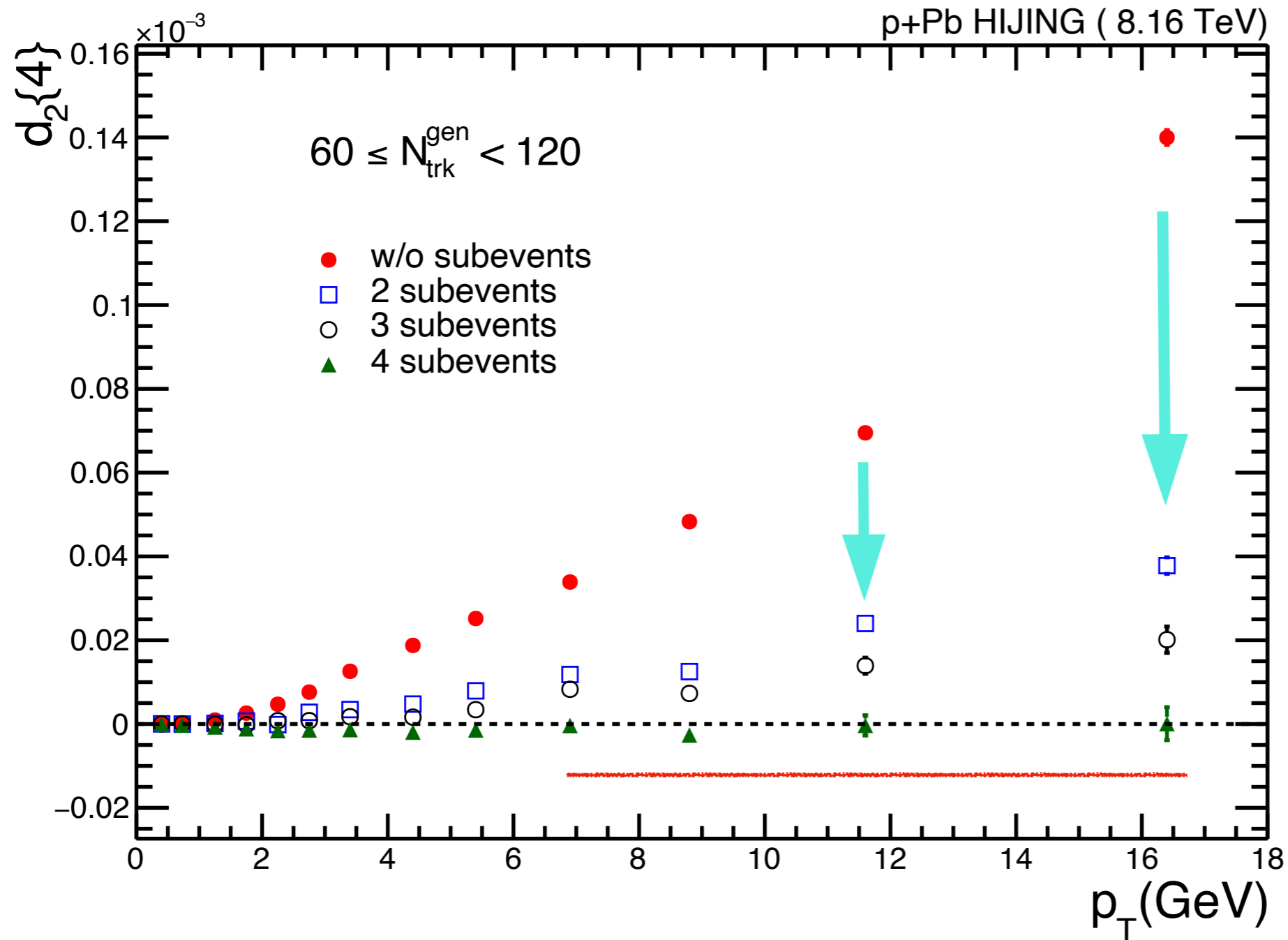
- **HIJING lacks collectivity** => used to cross check non-flow subtraction of subevent cumulant

✱  $d_2\{4\}$  in **HIJING** in  $60 \leq (N_{trk}^{gen}) < 120$



- **HIJING** lacks collectivity => used to cross check non-flow subtraction of subevent cumulant

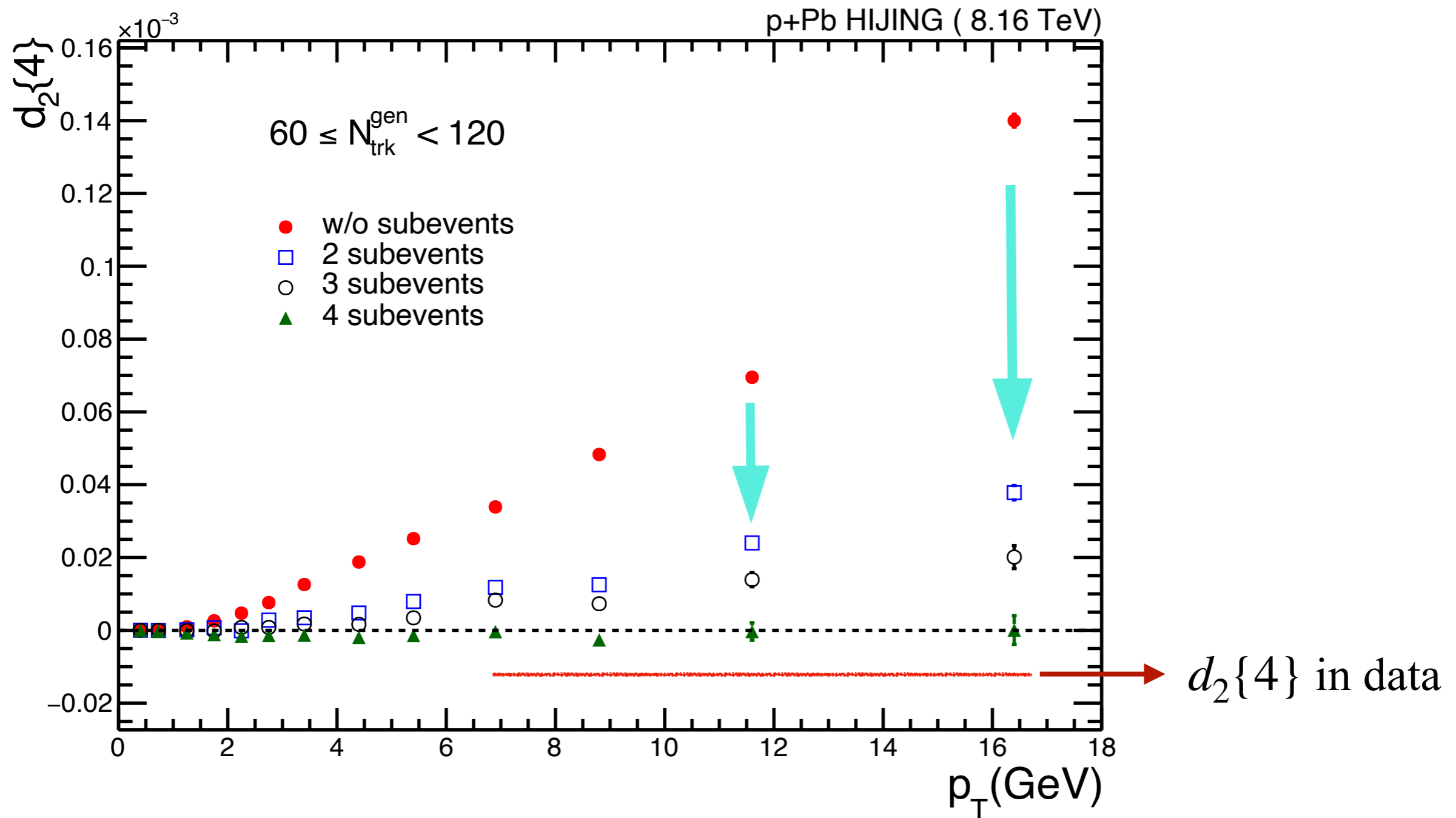
✱  $d_2\{4\}$  in **HIJING** in  $60 \leq (N_{trk}^{gen}) < 120$



- **HIJING** lacks collectivity => used to cross check non-flow subtraction of subevent cumulant

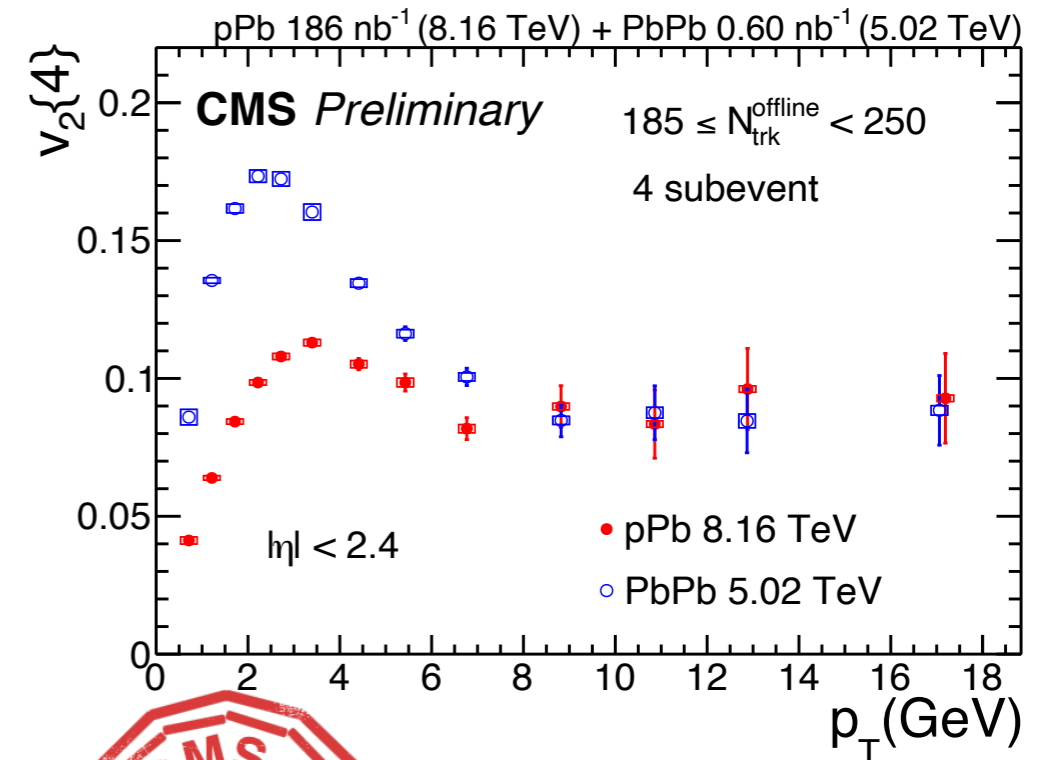


✱  $d_2\{4\}$  in **HIJING** in  $60 \leq (N_{trk}^{gen}) < 120$

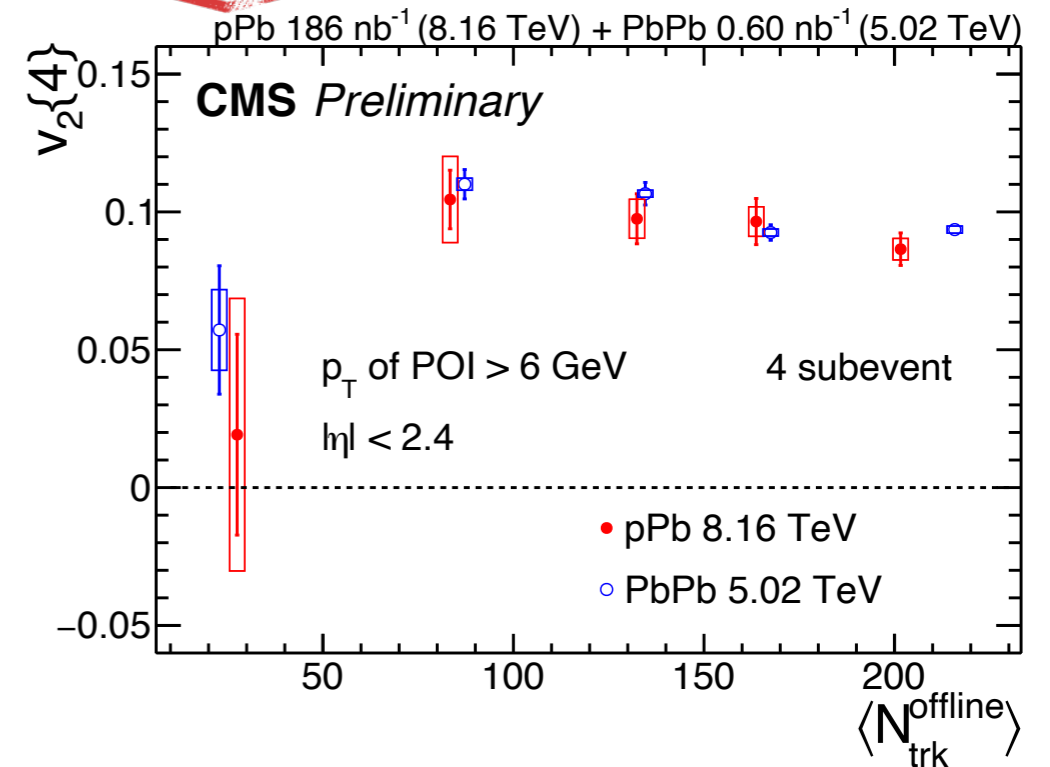


- **HIJING lacks collectivity** => used to cross check non-flow subtraction of subevent cumulant

- ❖ The results of  $v_2\{4\}$  with subevents for pPb & PbPb collisions at  $\sqrt{s_{NN}} = 8.16$  TeV &  $\sqrt{s_{NN}} = 5.02$  TeV, resp.
- ❖ After using subevent to remove nonflow, we have obtained a significant positive value for  $v_2\{4\}$  at high  $p_T$  in pPb
- ❖ A striking and surprising similarity in **high multiplicity pPb** and **peripheral PbPb collisions**
- ❖ These results provide new information on the interaction of high- $p_T$  partons with the medium in small system collisions

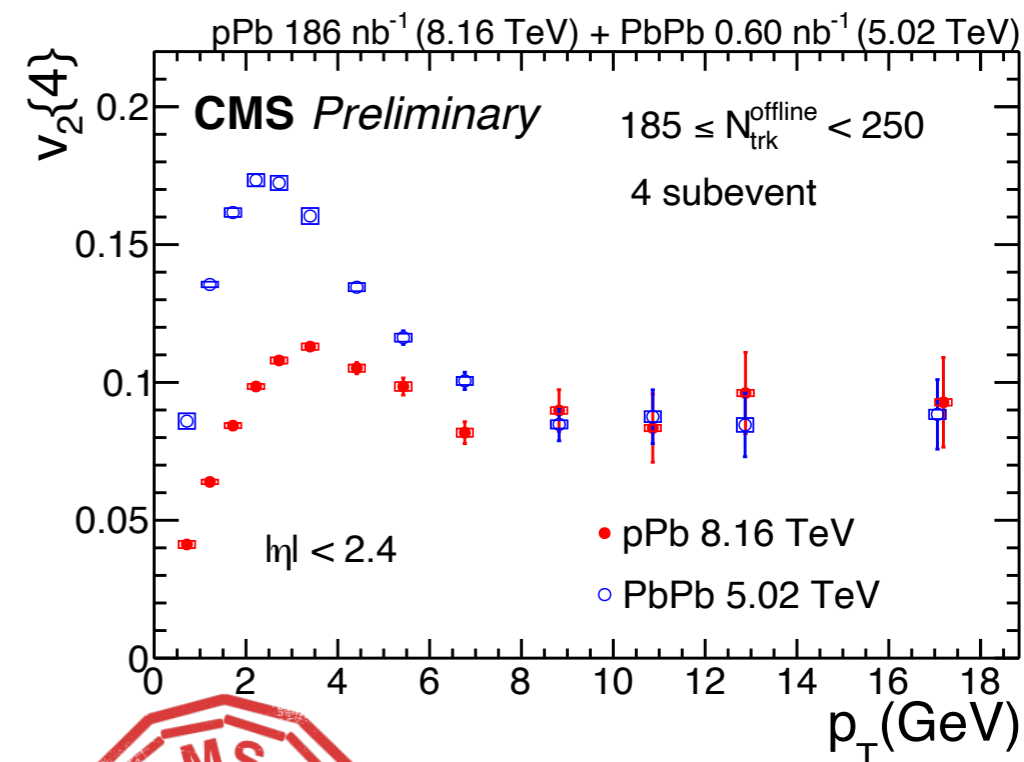


**CMS-PAS-HIN-23-002**

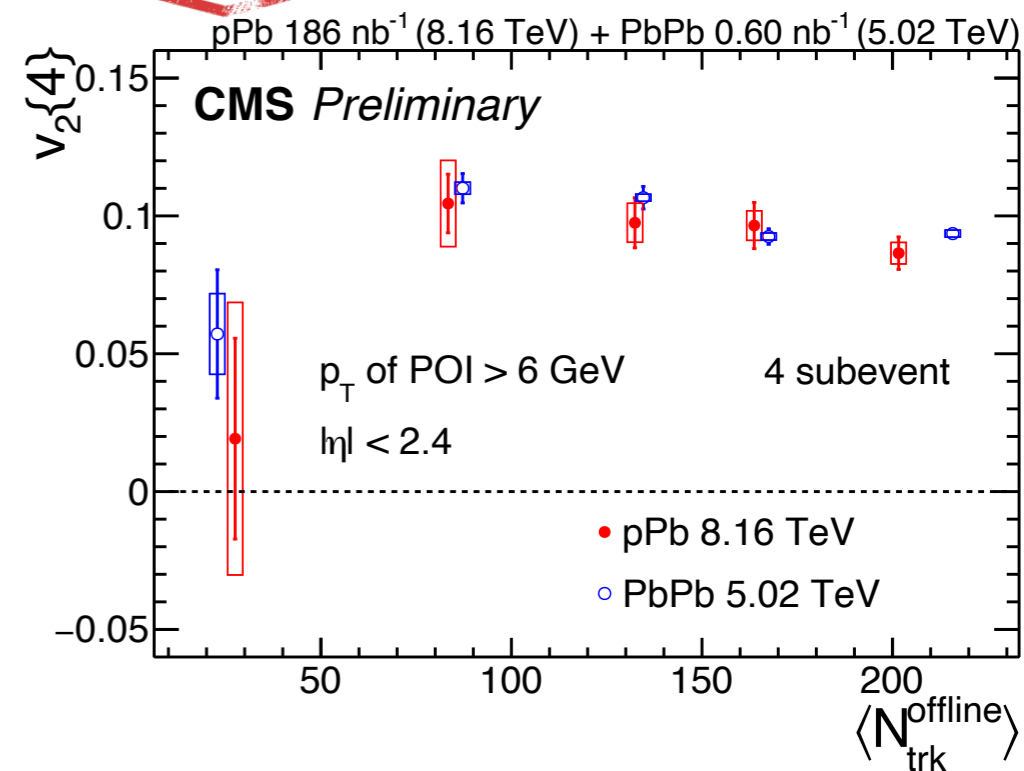


- ❖ The results of  $v_2\{4\}$  with subevents for pPb & PbPb collisions at  $\sqrt{s_{NN}} = 8.16$  TeV &  $\sqrt{s_{NN}} = 5.02$  TeV, resp.
- ❖ After using subevent to remove nonflow, we have obtained a significant positive value for  $v_2\{4\}$  at high  $p_T$  in pPb
- ❖ A striking and surprising similarity in **high multiplicity pPb** and **peripheral PbPb collisions**
- ❖ These results provide new information on the interaction of high- $p_T$  partons with the medium in small system collisions

ありがとう  
(Arigatō)



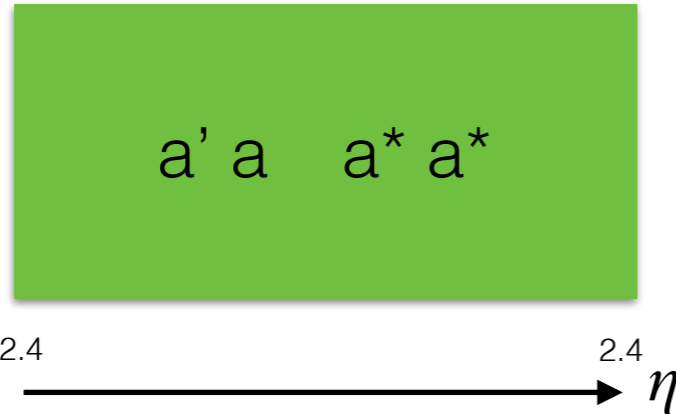
**CMS-PAS-HIN-23-002**



**BACK-UP**

## \* Differential cumulant $d_2\{4\}$ calculation in standard and 2 subevent method

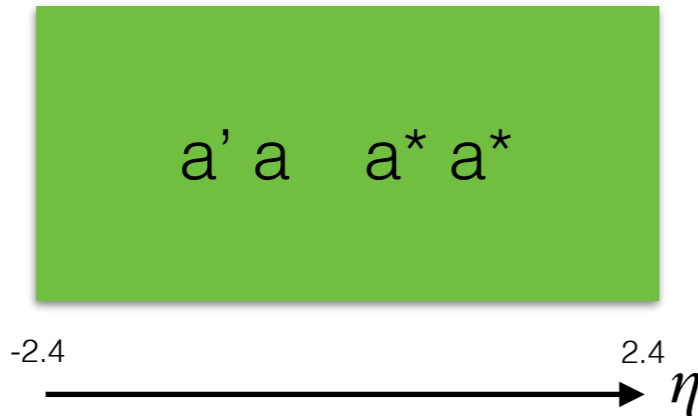
### ❖ Standard (w/o subevent)



$$d_n\{4\} = \langle\langle 4' \rangle\rangle - 2\langle\langle 2' \rangle\rangle \cdot \langle\langle 2 \rangle\rangle$$

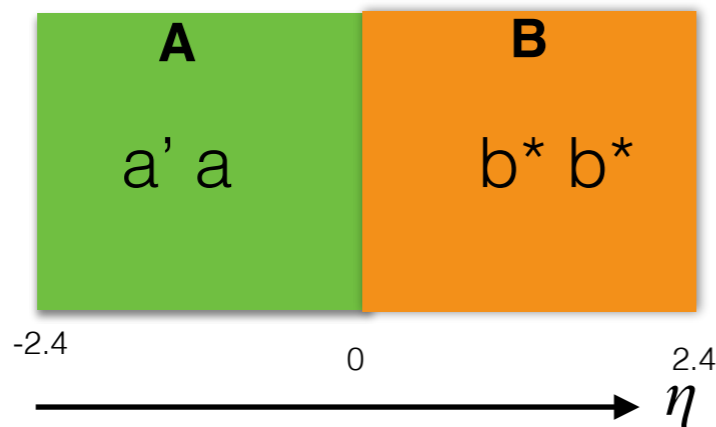
## \* Differential cumulant $d_2\{4\}$ calculation in standard and 2 subevent method

### ❖ Standard (w/o subevent)

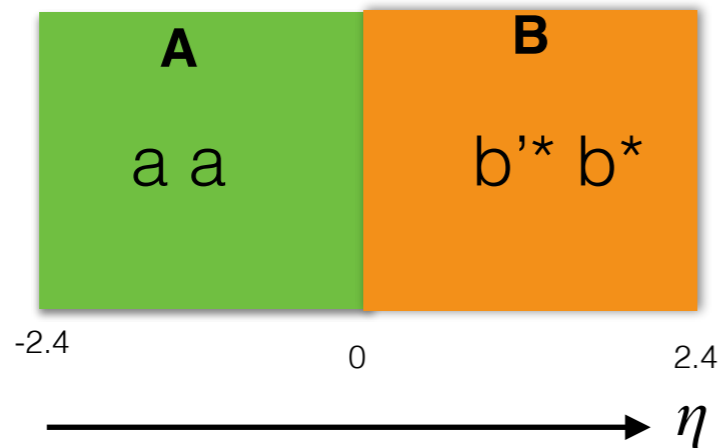


$$d_n\{4\} = \langle\langle 4' \rangle\rangle - 2\langle\langle 2' \rangle\rangle \cdot \langle\langle 2 \rangle\rangle$$

### ❖ 2 subevent



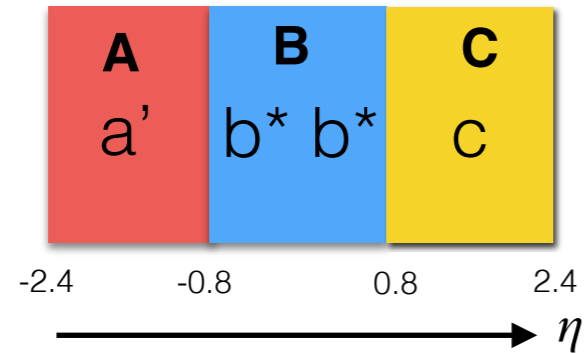
$$\longrightarrow d_n\{4\}_{2sub} = \langle\langle 4 \rangle^{a'a|bb}\rangle - 2\langle\langle 2 \rangle^{a'|b}\rangle \cdot \langle\langle 2 \rangle^{a|b}\rangle$$



$$\longrightarrow d_n\{4\}_{2sub} = \langle\langle 4 \rangle^{aa|b'b}\rangle - 2\langle\langle 2 \rangle^{a|b'}\rangle \cdot \langle\langle 2 \rangle^{a|b}\rangle$$

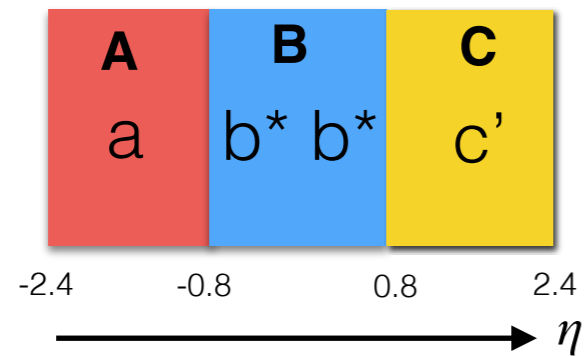
## \* Differential cumulant $d_2\{4\}$ calculation in 3 & 4 subevent method

### ❖ 3 subevent



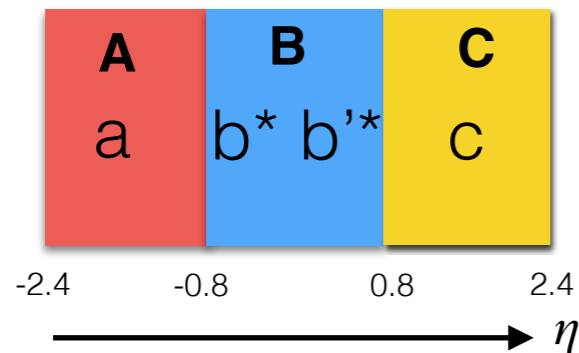
**POI :  $(-2.4 < \eta < 0.8)$**

$$\bullet d_n\{4\}_{3sub} = \langle\langle 4 \rangle^{a|bb|c}\rangle - 2\langle\langle 2 \rangle^{a|b}\rangle \cdot \langle\langle 2 \rangle^{b|c}\rangle$$



**POI :  $(0.8 < \eta < 2.4)$**

$$\bullet d_n\{4\}_{3sub} = \langle\langle 4 \rangle^{a|bb|c'}\rangle - 2\langle\langle 2 \rangle^{a|b}\rangle \cdot \langle\langle 2 \rangle^{b|c'}\rangle$$

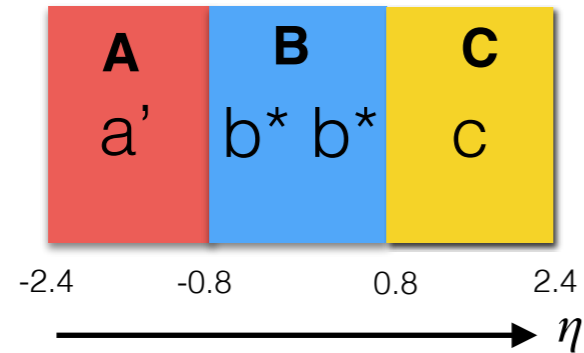


**POI :  $(-0.8 < \eta < 0.8)$**

$$\bullet d_n\{4\}_{3sub} = \langle\langle 4 \rangle^{a|bb'|c}\rangle - \langle\langle 2 \rangle^{a|b'}\rangle \cdot \langle\langle 2 \rangle^{b|c}\rangle - \langle\langle 2 \rangle^{a|b}\rangle \cdot \langle\langle 2 \rangle^{b'|c}\rangle$$

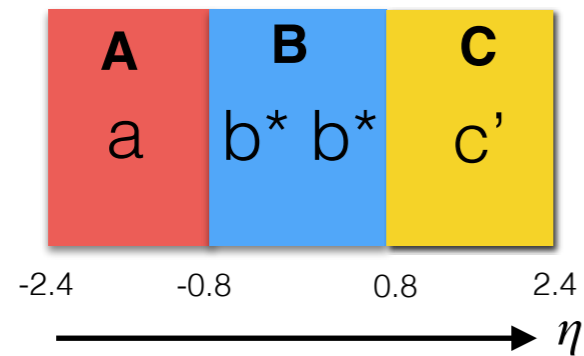
## \* Differential cumulant $d_2\{4\}$ calculation in 3 & 4 subevent method

### ❖ 3 subevent



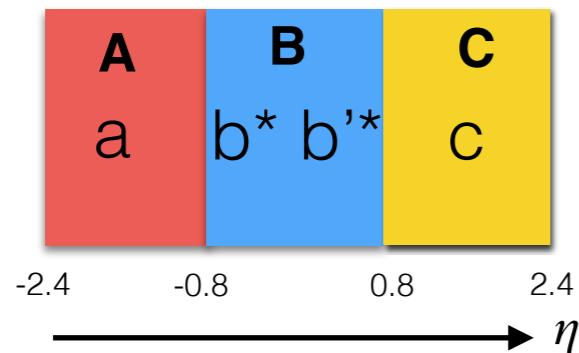
**POI :  $(-2.4 < \eta < 0.8)$**

$$\bullet d_n\{4\}_{3sub} = \langle\langle 4 \rangle^{a|bb|c}\rangle - 2\langle\langle 2 \rangle^{a|b}\rangle \cdot \langle\langle 2 \rangle^{b|c}\rangle$$



**POI :  $(0.8 < \eta < 2.4)$**

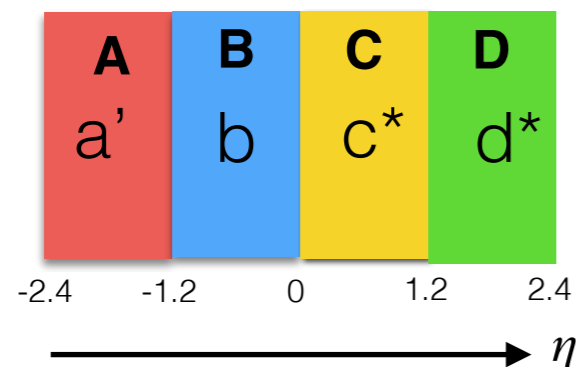
$$\bullet d_n\{4\}_{3sub} = \langle\langle 4 \rangle^{a|bb|c'}\rangle - 2\langle\langle 2 \rangle^{a|b}\rangle \cdot \langle\langle 2 \rangle^{b|c'}\rangle$$



**POI :  $(-0.8 < \eta < 0.8)$**

$$\bullet d_n\{4\}_{3sub} = \langle\langle 4 \rangle^{a|bb'|c}\rangle - \langle\langle 2 \rangle^{a|b'}\rangle \cdot \langle\langle 2 \rangle^{b|c}\rangle - \langle\langle 2 \rangle^{a|b}\rangle \cdot \langle\langle 2 \rangle^{b'|c}\rangle$$

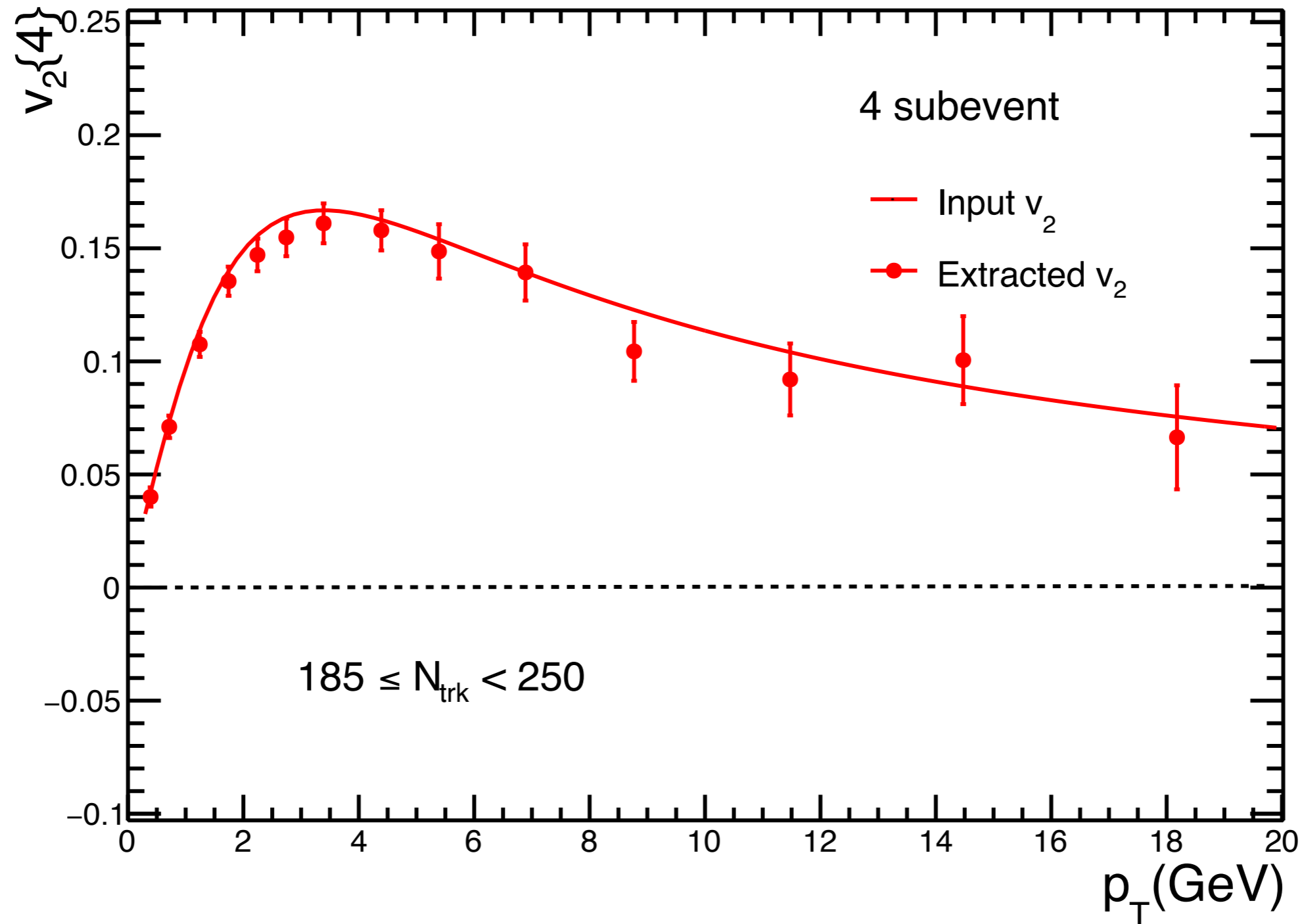
### ❖ 4 subevent



$$d_n\{4\}_{4sub} = \langle\langle 4 \rangle^{a'|b|c|d}\rangle - \langle\langle 2 \rangle^{a'|c}\rangle \cdot \langle\langle 2 \rangle^{b|d}\rangle - \langle\langle 2 \rangle^{a'|d}\rangle \cdot \langle\langle 2 \rangle^{b|c}\rangle$$



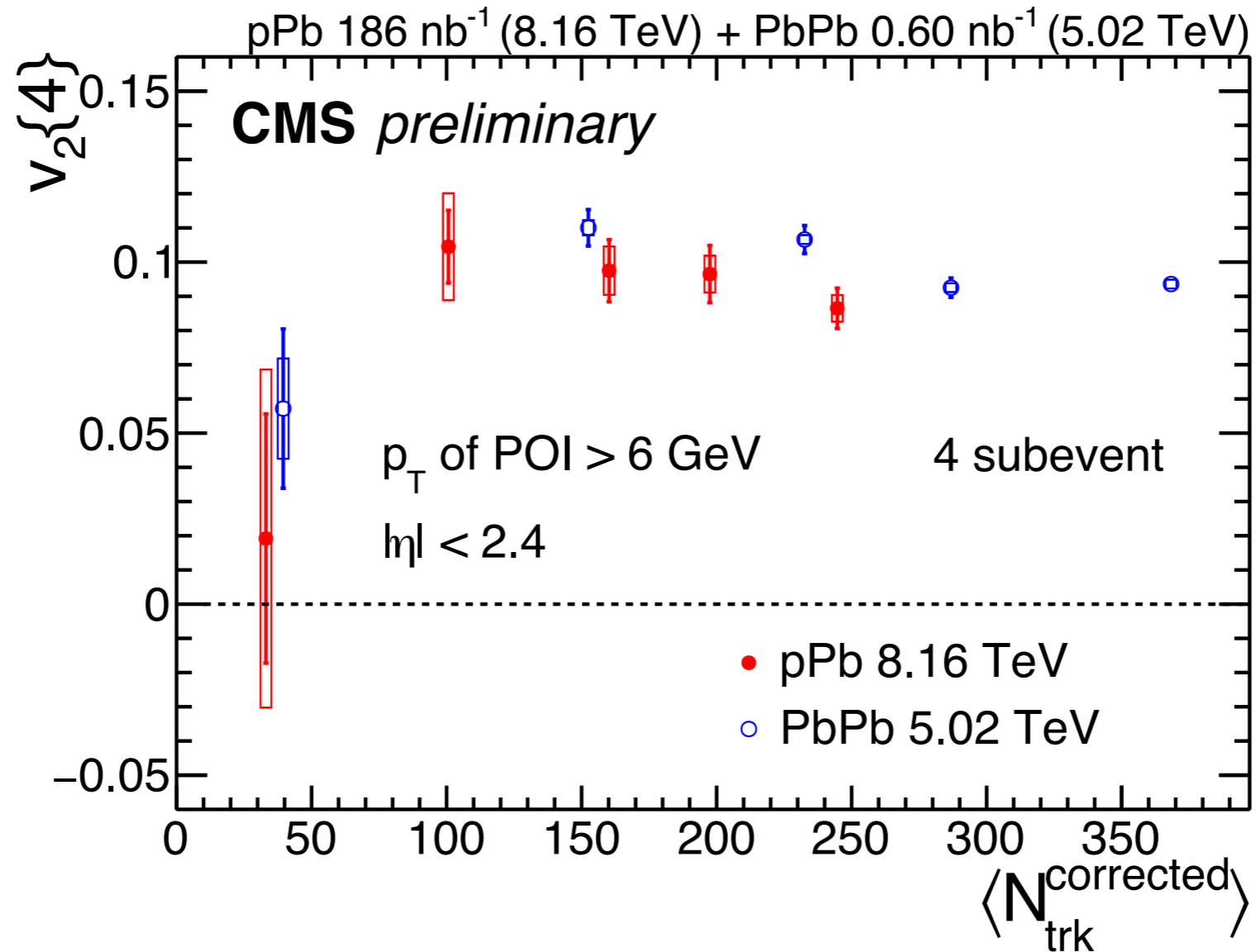
## \* $v_2\{4\}$ with toy model simulation



- Able to extract almost all input  $v_2$  with 4 subevent

# Supplementary plot

✱  $v_2\{4\}$  in different  $N_{trk}^{corrected}$  bins with POI  $p_T > 6$  GeV



$N_{trk}^{offline}$ range	pPb		PbPb	
	$\langle N_{trk}^{offline} \rangle$	$\langle N_{trk}^{corrected} \rangle$	$\langle N_{trk}^{offline} \rangle$	$\langle N_{trk}^{corrected} \rangle$
(0, 60)	27	$33 \pm 1$	23	$39 \pm 2$
[60, 120)	83	$101 \pm 4$	87	$152 \pm 6$
[120, 150)	132	$160 \pm 6$	135	$233 \pm 10$
[150, 185)	164	$198 \pm 7$	168	$287 \pm 12$
[185, 250)	202	$245 \pm 10$	216	$368 \pm 16$